

1 Event History Analysis for psychological time-to-event data: A tutorial in R with examples  
2 in Bayesian and frequentist workflows

3 Sven Panis<sup>1</sup> & Richard Ramsey<sup>1</sup>

4 <sup>1</sup> ETH Zürich

5 Author Note

6 Neural Control of Movement lab, Department of Health Sciences and Technology  
7 (D-HEST). Social Brain Sciences lab, Department of Humanities, Social and Political  
8 Sciences (D-GESS).

9 The authors made the following contributions. Sven Panis: Conceptualization,  
10 Writing - Original Draft Preparation, Writing - Review & Editing; Richard Ramsey:  
11 Conceptualization, Writing - Review & Editing, Supervision.

12 Correspondence concerning this article should be addressed to Sven Panis, ETH  
13 GLC, room G16.2, Gloriastrasse 37/39, 8006 Zürich. E-mail: sven.panis@hest.ethz.ch

14

## Abstract

15 Time-to-event data such as response times, saccade latencies, and fixation durations form a  
16 cornerstone of experimental psychology, and have had a widespread impact on our  
17 understanding of human cognition. However, the orthodox method for analysing such data  
18 – comparing means between conditions – is known to conceal valuable information about  
19 the timeline of psychological effects, such as their onset time and duration. The ability to  
20 reveal finer-grained, “temporal states” of cognitive processes can have important  
21 consequences for theory development by qualitatively changing the key inferences that are  
22 drawn from psychological data. Luckily, well-established analytical approaches, such as  
23 event history analysis (EHA), are able to evaluate the detailed shape of time-to-event  
24 distributions, and thus characterise the time course of psychological states. One barrier to  
25 wider use of EHA, however, is that the analytical workflow is typically more  
26 time-consuming and complex than orthodox approaches. To help achieve broader uptake,  
27 in this paper we outline a set of tutorials that detail how to implement one distributional  
28 method known as discrete-time EHA. We illustrate how to wrangle raw data files and  
29 calculate descriptive statistics, as well as how to calculate inferential statistics via Bayesian  
30 and frequentist multilevel regression modelling. Along the way, we touch upon several key  
31 aspects of the workflow, such as how to specify regression models, the implications for  
32 experimental design, as well as how to manage inter-individual differences. We finish the  
33 article by considering the benefits of the approach for understanding psychological states,  
34 as well as the limitations and future directions of this work. Finally, the project is written  
35 in R and freely available, which means the general approach can easily be adapted to other  
36 data sets, and all of the tutorials are available as .html files to widen access beyond R-users.

37       *Keywords:* response times, event history analysis, Bayesian multi-level regression  
38 models, experimental psychology, cognitive psychology

39 Word count: X

40

## 1. Introduction

### 41 1.1 Motivation and background context: Comparing means versus 42 distributional shapes

43 In experimental psychology, it is standard practice to analyse response times (RTs),  
44 saccade latencies, and fixation durations by calculating average performance across a series  
45 of trials. Such mean-average comparisons have been the workhorse of experimental  
46 psychology over the last century, and have had a substantial impact on theory development  
47 as well as our understanding of the structure of cognition and brain function. However,  
48 differences in mean RT conceal important pieces of information, such as when an  
49 experimental effect starts, how long it lasts, how it evolves with increasing waiting time,  
50 and whether its onset is time-locked to other events (Panis, 2020; Panis, Moran,  
51 Wolkersdorfer, & Schmidt, 2020; Panis & Schmidt, 2016, 2022; Panis, Torfs, Gillebert,  
52 Wagemans, & Humphreys, 2017; Panis & Wagemans, 2009; Wolkersdorfer, Panis, &  
53 Schmidt, 2020). Such information is useful not only for the interpretation of experimental  
54 effects under investigation, but also for cognitive psychophysiology and computational  
55 model selection (Panis, Schmidt, Wolkersdorfer, & Schmidt, 2020).

56 As a simple illustration, Figure 1 shows the results of several simulated RT data sets,  
57 which show how mean-average comparisons between two conditions can conceal the shape  
58 of the underlying RT distributions. For instance, in examples 1-3, mean RT is always  
59 comparable between two conditions, while the distributions differ (Figure 1, left). In  
60 contrast, in examples 4-6, mean RT is lower in condition 2 compared to condition 1, but  
61 the RT distributions differ in each case (Figure 1, right). Therefore, a comparison of means  
62 would lead to a similar conclusion in examples 1-3, as well as examples 4-6, whereas a  
63 comparison of the distributions would lead to a different conclusion in every case.

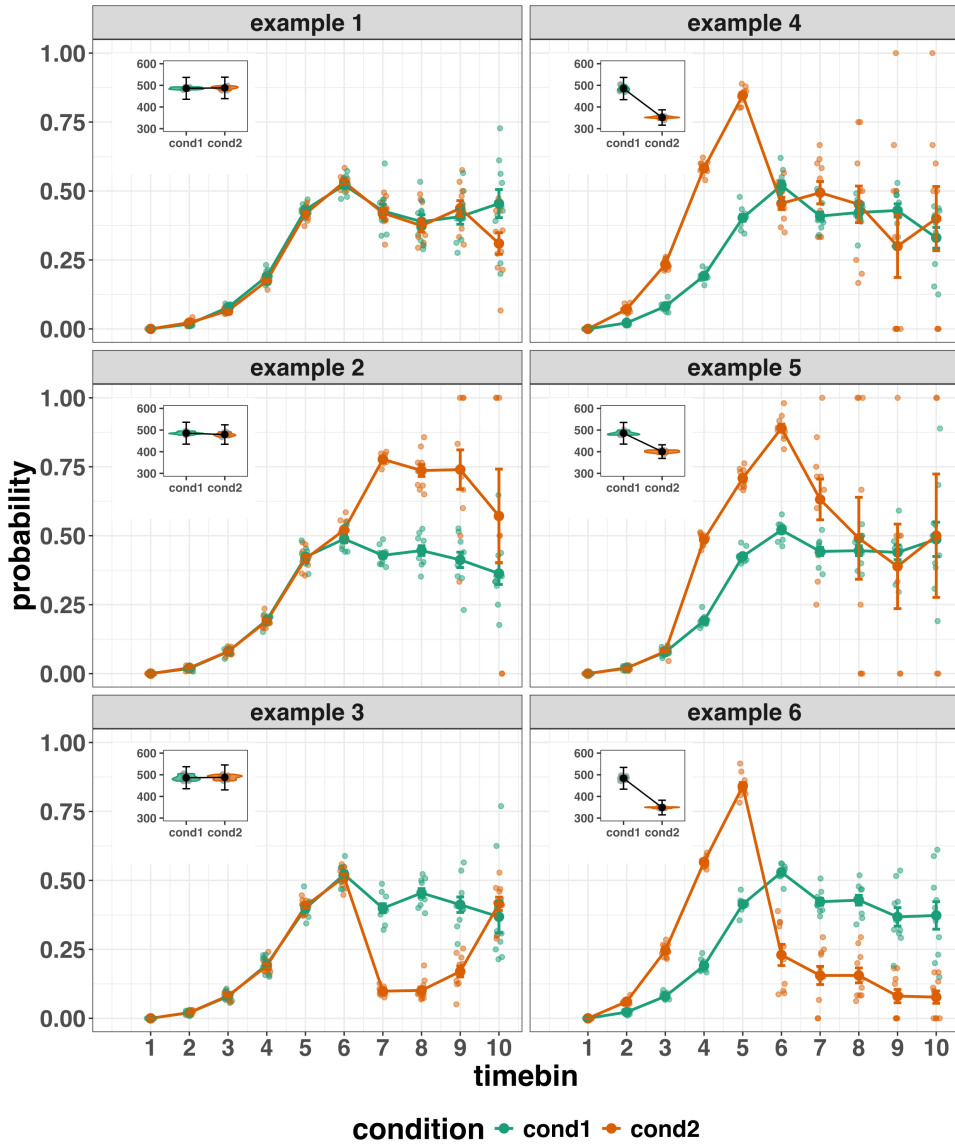


Figure 1. Means versus distributional shapes for six different simulated data set examples.

The first second after stimulus onset is divided in ten bins of 100 ms. Timebin indicates the bin rank. The first bin is (0,100], the last bin is (900,1000]. For our purposes here, it is enough to know that the distributions plotted represent the probability of an event occurring in that timebin, given that it has not yet occurred. Insets show mean response time per condition.

65 data across trials, a distributional approach offers the possibility to reveal the time course  
66 of psychological states. As such, the approach permits different kinds of questions to be  
67 asked, different inferences to be made, and it holds the potential to discriminate between  
68 different theoretical accounts of psychological and/or brain-based processes. For example,  
69 the distributions in Example 4 show that the effect starts between 100 and 200 ms (in  
70 timebin 2) and is gone when the waiting time reaches 500 ms or more. In contrast, in  
71 Example 5, the effect starts around 300 ms and is gone by 700 ms. And in the Example 6,  
72 the effect reverses between 500 and 600 ms. What kind of theory or theories could account  
73 for such effects? Are there new auxiliary assumptions that theories need to adopt? And are  
74 there new experiments that need to be performed to test the novel predictions that follow  
75 from these analyses? As we show later using published examples, for many psychological  
76 questions, such “temporal states” information can be theoretically meaningful by leading to  
77 more fine-grained understanding of psychological processes, as well as adding a relatively  
78 under-used dimension – the passage of time – to the theory building toolkit.

79 From a historical perspective, it is worth noting that the development of analytical  
80 tools that can estimate or predict whether and when events will occur is not a new  
81 endeavour. Indeed, hundreds of years ago, analytical methods were developed to predict  
82 the duration of time until people died (e.g., Halley, 1997; Makeham, 1860). The same logic  
83 has been applied to psychological time-to-event data, as previously demonstrated (Panis,  
84 Schmidt, et al., 2020).

## 85 1.2 Aims and structure of the paper

86 In this paper, we focus on a distributional method for time-to-event data known as  
87 discrete-time Event History Analysis (EHA), a.k.a. survival analysis, hazard analysis,  
88 duration analysis, failure-time analysis, and transition analysis (Singer & Willett, 2003).  
89 We hope to show the value of EHA for knowledge and theory building in cognitive  
90 psychology and related areas of research, such as cognitive neuroscience. Most importantly,

91 we provide tutorials that provide step-by-step code and instructions in the hope that we  
92 can enable others to use EHA in a more routine, efficient and effective manner.

93 We first provide a brief overview of EHA to orient the reader to the basic concepts  
94 that we will use throughout the paper. However, this will remain relatively short, as this  
95 has been covered in detail before (Allison, 1982, 2010; Singer & Willett, 2003). Indeed, our  
96 primary aim here is to introduce the set of tutorials, which explain **how** to do such  
97 analyses, rather than repeat in any detail **why** you may do them.

98 We provide six different tutorials, which are written in the R programming language  
99 and publicly available on our Github and the Open Science Framework (OSF) pages, along  
100 with all of the other code and material associated with the project. The tutorials provide  
101 hands-on, concrete examples of key parts of the analytical process, so that others can apply  
102 EHA to their own time-to-event data sets. Each tutorial is provided as an RMarkdown file,  
103 so that others can download and adapt the code to fit their own purposes. Additionally,  
104 each tutorial is made available as a .html file, so that it can be viewed by any web browser,  
105 and thus available to those that do not use R. Finally, the manuscript itself is written in R  
106 using the papaja package (Aust & Barth, 2024), which makes it computationally  
107 reproducible, in terms of the underlying data and figures.

108 In Tutorial 1a, we illustrate how to process or “wrangle” a previously published RT +  
109 accuracy data set to calculate descriptive statistics when there is one independent variable.  
110 The descriptive statistics are plotted, and we comment on their interpretation. In Tutorial  
111 1b we provide a generalisation of this approach to illustrate how one can calculate the  
112 descriptive statistics when using a more complex design, such as when there are two  
113 independent variables.

114 In Tutorial 2a, we illustrate how one can fit Bayesian multi-level regression models to  
115 RT data using the R package brms. We also perform prior predictive checks, compare  
116 models, and interpret the plots of the predicted hazard functions for the selected model,

117 and the posterior distributions of our contrasts of interest. In Tutorial 2b we fit Bayesian  
118 multi-level regression models to *timed* accuracy data to perform a micro-level  
119 speed-accuracy tradeoff (SAT) analysis, which complements the EHA of RT data for choice  
120 RT data.

121 In Tutorial 3a, we shortly illustrate how to fit similar multilevel regression models for  
122 RT data in a frequentist framework using the R package lme4. We then briefly compare  
123 and contrast these inferential frameworks when applied to EHA. In Tutorial 3b, we  
124 illustrate how to perform the SAT analysis in a frequentist framework.

125 In tutorial 4, we illustrate one approach to planning how much data to collect in an  
126 experiment using EHA. We use data simulation techniques to vary sample size and trial  
127 count per condition until a certain degree of statistical power or precision is reached.  
128 [[more to come here, once we have written the tutorial]].

129 In summary, even though EHA is a widely used statistical tool and there already exist  
130 many excellent reviews (e.g., Blossfeld & Rohwer, 2002; Box-Steffensmeier, 2004; Hosmer,  
131 Lemeshow, & May, 2011; Teachman, 1983) and tutorials (e.g., Allison, 2010; Landes,  
132 Engelhardt, & Pelletier, 2020) on its general use-cases, we are not aware of any tutorials  
133 that are aimed at psychological time-to-event data, and which provide worked examples of  
134 the key data processing and multi-level regression modelling steps. Therefore, our ultimate  
135 goal is twofold: first, we want to convince readers of the many benefits of using EHA when  
136 dealing with time-to-event data with a focus on psychological time-to-event data, and  
137 second, we want to provide a set of practical tutorials, which provide step-by-step  
138 instructions on how you actually perform a discrete-time EHA on time-to-event data such  
139 as RT data, as well as a complementary discrete-time SAT analysis on timed accuracy data.

**2. A brief introduction to event history analysis**

For a comprehensive background context to EHA, we recommend several excellent textbooks (Allison, 2010; Singer & Willett, 2003). Likewise, for a general introduction to understanding regression equations, we recommend several excellent textbooks (Gelman, Hill, & Vehtari, 2020; Winter, 2019). Our focus here is not on providing a detailed account of the underlying regression equations, since this topic has been comprehensively covered many times before. Instead, we want to provide an intuition regarding how EHA works in general, as well as in the context of experimental psychology. As such, we only supply regression equations in the supplementary material.

**2.1 Basic features of event history analysis**

To apply EHA, one must be able to:

1. define an event of interest that represents a qualitative change that can be situated in time (e.g., a button press, a saccade onset, a fixation offset, etc.);
2. define time point zero (e.g., target stimulus onset, fixation onset, etc.);
3. measure the passage of time between time point zero and event occurrence in discrete or continuous time units.

In EHA, the definition of hazard and the type of models employed depend on whether one is using continuous or discrete time units. Since our focus here is on hazard models that use discrete time units, we describe that approach. After dividing time in discrete, contiguous time bins indexed by  $t$  (e.g.,  $t = 1:10$  timebins), let  $RT$  be a discrete random variable denoting the rank of the time bin in which a particular person's response occurs in a particular experimental condition. For example, the first response might occur at 546 ms and it would be in timebin 6 (any RTs from 501 ms to 600 ms).

163 Discrete-time EHA focuses on the discrete-time hazard function of event occurrence

164 and the discrete-time survivor function (Figure 2). The equations that define both of these

165 functions are reported in part A of the supplementary material. The discrete-time hazard

166 function gives you, for each time bin, the probability that the event occurs (sometime) in

167 bin  $t$ , given that the event does not occur in previous bins. In other words, it reflects the

168 instantaneous likelihood that the event occurs in the current bin, given that it has not yet

169 occurred in the past, i.e., in one of the prior bins. In contrast, the discrete-time survivor

170 function cumulates the bin-by-bin risks of event *nonoccurrence* to obtain the survival

171 probability, the probability that the event occurs after bin  $t$ . In other words, the survivor

172 function gives you for each time bin the likelihood that the event occurs in the future, i.e.,

173 in one of the subsequent timebins.

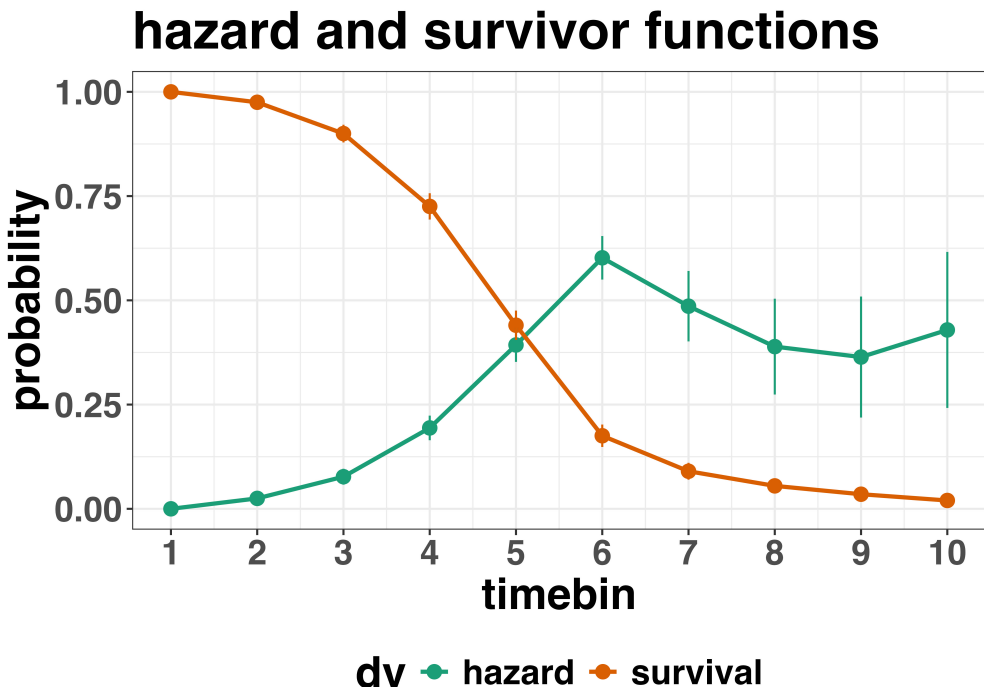


*Figure 2.* Discrete-time hazard and survivor functions. Discrete time-to-event data were simulated for 200 trials of 1 experimental condition. While the hazard function is the vehicle for inferring the time course of cognitive processes, the survival probability  $S(t-1)$  can help to qualify or provide context to the interpretation of the hazard probability  $h(t)$ . For example, the high hazard of  $.60 = h(t=6)$  is experienced only by 44 percent of the trials, as  $S(t=5) = .44$ . Because the survivor function is a decreasing function of time, the error bars in later parts of the hazard function will always be wider and less precise compared to earlier parts.

<sup>174</sup> **2.2 Benefits of event history analysis**

<sup>175</sup> Statisticians and mathematical psychologists recommend focusing on the hazard  
<sup>176</sup> function when analyzing time-to-event data for various reasons. We do not cover these  
<sup>177</sup> benefits in detail here, as these are more general topics that have been covered elsewhere in  
<sup>178</sup> textbooks. Instead, we briefly summarise list the benefits below, and refer the reader to  
<sup>179</sup> section F of Supplementary Materials for more detailed coverage of the benefits. A  
<sup>180</sup> summary of the benefits are as follows:

- 181 1. Hazard functions are more diagnostic than density functions when one is interested in  
182 studying the detailed shape of a RT distribution (Holden et al., 2009).
- 183 2. RT distributions may differ from each other in multiple ways, and hazard functions  
184 allow one to capture these differences which mean-average comparisons may conceal  
185 (Townsend, 1990).
- 186 3. EHA takes account of more of the data collected in a typical speeded response  
187 experiment, by virtue of not discarding right-censored observations. Trials with very  
188 long RTs are not discarded, but instead contribute to the risk set in each time bin  
189 (see below).
- 190 4. Hazard modeling allows one to incorporate time-varying explanatory covariates, such  
191 as heart rate, electroencephalogram (EEG) signal amplitude, gaze location, etc.  
192 (Allison, 2010). This is useful for linking physiological effects to behavioral effects  
193 when performing cognitive psychophysiology (Meyer, Osman, Irwin, & Yantis, 1988).
- 194 5. EHA can help to solve the problem of model mimicry, i.e., the fact that different  
195 computational models can often predict the same mean RTs as observed in the  
196 empirical data, but not necessarily the detailed shapes of the empirical RT hazard  
197 distributions. As such, EHA can be a tool to help distinguish between competing  
198 theories of cognition and brain function.

### 199 2.3 Event history analysis in the context of experimental psychology

200 To make EHA more relevant to researchers studying cognitive psychology and

201 cognitive neuroscience, in this section we provide a relevant worked example and consider  
202 implications that are relevant to that domain of research.

203 **2.3.1 A worked example.** In the context of experimental psychology, it is

204 common for participants to be presented with either a 1-button detection task or a

discrimination task. For example, a task may involve choosing between two response options with only one of them being correct. For such two-choice RT data, the discrete-time EHA of the RT data (hazard and survivor functions) can be extended with a discrete-time SAT analysis of the timed accuracy data. Specifically, the hazard function of event occurrence can be extended with the discrete-time conditional accuracy function, which gives you the probability that a response is correct given that it is emitted in time bin  $t$  (Allison, 2010; Kantowitz & Pachella, 2021; Wickelgren, 1977). We refer to this extended (hazard + conditional accuracy) analysis for choice RT data as EHA/SAT.

Integrating results between hazard and conditional accuracy functions for choice RT data can be informative for understanding psychological processes. To illustrate, we consider a hypothetical choice RT example that is inspired by real data (Panis & Schmidt, 2016), but simplified to make the main point clearer (Figure 3). In a standard priming paradigm, there is a prime stimulus (e.g., an arrow pointing left or right) followed by a target stimulus (another arrow pointing left or right). The prime can then be congruent or incongruent with the target.

Figure 3 shows that the early upswing in hazard is equal for both priming conditions, and that early emitted responses are always correct in the congruent condition and always incorrect in the incongruent condition. These results show that for short waiting times (< timebin 6), responses always follow the prime (and not the target, as instructed). During timebin 6 the target-triggered response channel is activated and causes response competition –  $ca(6) = .5$  – and a lower hazard probability in the incongruent condition. For waiting times of 600 ms or more, the hazard of response occurrence is lower in incongruent compared to congruent trials, and all responses emitted in these late bins are correct.

This joint pattern of results is interesting because it can provide meaningfully different conclusions about psychological processes compared to conventional analyses, such as computing mean-average RT and accuracy across trials. Mean-average RT would only

<sup>231</sup> represent the overall ability of cognition to overcome interference, on average, across trials.  
<sup>232</sup> For instance, if mean-average RT was higher in incongruent than congruent trials, one may  
<sup>233</sup> conclude that cognitive mechanisms that support interference control are working as  
<sup>234</sup> expected across trials, and are indexed by each recorded response. But such a conclusion is  
<sup>235</sup> not supported when the effects are explored over a timeline. Instead, the psychological  
<sup>236</sup> conclusion is much more nuanced and suggests that multiple states start, stop and possibly  
<sup>237</sup> interact over a particular temporal window.

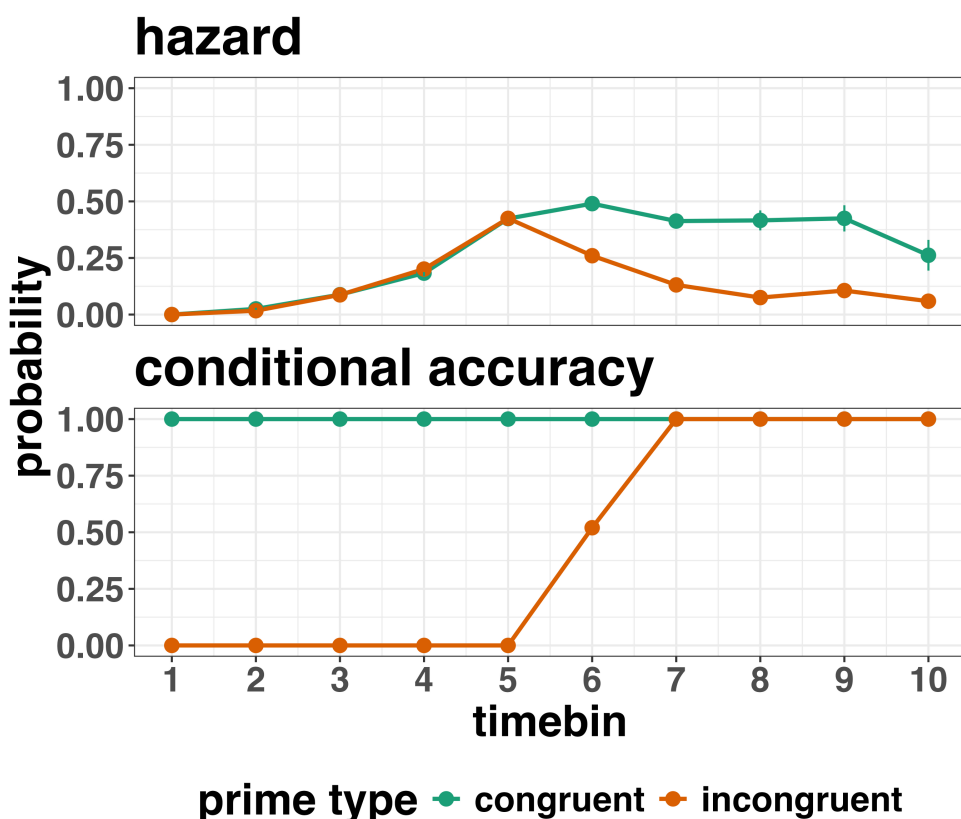


*Figure 3.* Discrete-time hazard and conditional accuracy functions. Discrete time-to-event and conditional accuracy data were simulated for 2000 trials for each of two priming conditions (congruent and incongruent prime stimuli). Bin width equals 100 ms.

<sup>238</sup> Unlocking the temporal states of cognitive processes can be revealing for theory  
<sup>239</sup> development and the understanding of basic psychological processes. Possibly more

240 importantly, however, is that it simultaneously opens the door to address many new and  
241 previously unanswered questions. Do all participants show similar temporal states or are  
242 there individual differences? Do such individual differences extend to those individuals that  
243 have been diagnosed with some form of psychopathology? How do temporal states relate to  
244 brain-based mechanisms that might be studied using other methods from cognitive  
245 neuroscience? And how much of theory in cognitive psychology would be in need of  
246 revision if mean-average comparisons were supplemented with a temporal states approach?

247 **2.3.2 Implications for designing experiments.** Performing EHA in  
248 experimental psychology has implications for how experiments are designed. Indeed, if  
249 trials are categorised as a function of when responses occur, then each timebin will only  
250 include a subset of the total number of trials. For example, let's consider an experiment  
251 where each participant performs 2 conditions and there are 100 trial repetitions per  
252 condition. Those 100 trials must be distributed in some manner across the chosen number  
253 of bins.

254 In such experimental designs, since the number of trials per condition are spread  
255 across bins, it is important to have a relatively large number of trial repetitions per  
256 participant and per condition. Accordingly, experimental designs using this approach  
257 typically focus on factorial, within-subject designs, in which a large number of observations  
258 are made on a relatively small number of participants (so-called small- $N$  designs). This  
259 approach emphasizes the precision and reproducibility of data patterns at the individual  
260 participant level to increase the inferential validity of the design (Baker et al., 2021; Smith  
261 & Little, 2018).

262 In contrast to the large- $N$  design that typically average across many participants  
263 without being able to scrutinize individual data patterns, small- $N$  designs retain crucial  
264 information about the data patterns of individual observers. This can be advantageous  
265 whenever participants differ systematically in their strategies or in the time courses of their  
266 effects, so that averaging them would lead to misleading data patterns. Note that because

267 statistical power derives both from the number of participants and from the number of  
268 repeated measures per participant and condition, small- $N$  designs can still achieve what  
269 are generally considered acceptable levels of statistical power, if they have a sufficient  
270 amount of data overall (Baker et al., 2021; Smith & Little, 2018).

271 **3. An overview of the general analytical workflow**

272 Although the focus is on EHA/SAT, we also want to briefly comment on broader  
273 aspects of our general analytical workflow, which relate more to data science and data  
274 analysis workflows.

275 **3.1 Data science workflow and descriptive statistics**

276 We perform data wrangling following tidyverse principles and a functional  
277 programming approach (Wickham, Çetinkaya-Rundel, & Grolemund, 2023). Functional  
278 programming basically means you don't write your own loops but instead use functions  
279 that have been built and tested by others. [[more here, as necessary]].

280 **3.2 Inferential statistical approach**

281 Our lab adopts a estimation approach to multi-level regression (Kruschke & Liddell,  
282 2018; Winter, 2019), which is heavily influenced by the Bayesian framework as suggested  
283 by Richard McElreath (Kurz, 2023b; McElreath, 2018). We also use a “keep it maximal”  
284 approach to specifying varying (or random) effects (Barr, Levy, Scheepers, & Tily, 2013).  
285 This means that wherever possible we include varying intercepts and slopes per participant  
286 To make inferences, we use two main approaches. We compare models of different  
287 complexity, using information criteria (e.g., WAIC) and cross-validation (e.g., LOO), to  
288 evaluate out-of-sample predictive accuracy (McElreath, 2018). We also take the most  
289 complex model and evaluate key parameters of interest using point and interval estimates.

<sup>290</sup> **3.3 Implementation**

<sup>291</sup> We used R (Version 4.4.0; R Core Team, 2024)<sup>1</sup> for all reported analyses. The  
<sup>292</sup> content of the tutorials, in terms of EHA and multi-level regression modelling, is mainly  
<sup>293</sup> based on Allison (2010), Singer and Willett (2003), McElreath (2018), Heiss (2021), Kurz  
<sup>294</sup> (2023a), and Kurz (2023b).

<sup>295</sup> **4. Tutorials**

<sup>296</sup> Tutorials 1a and 1b show how to calculate and plot the descriptive statistics of  
<sup>297</sup> EHA/SAT when there are one and two independent variables, respectively. Tutorials 2a  
<sup>298</sup> and 2b illustrate how to use Bayesian multilevel modeling to fit hazard and conditional  
<sup>299</sup> accuracy models, respectively. Tutorials 3a and 3b show how to implement, respectively,  
<sup>300</sup> multilevel models for hazard and conditional accuracy in the frequentist framework.  
<sup>301</sup> Additionally, to further simplify the process for other users, the first two tutorials rely on a  
<sup>302</sup> set of our own custom functions that make sub-processes easier to automate, such as data  
<sup>303</sup> wrangling and plotting functions (see part B in the supplemental material for a list of the

---

<sup>1</sup> We, furthermore, used the R-packages *bayesplot* (Version 1.11.1; Gabry, Simpson, Vehtari, Betancourt, & Gelman, 2019), *brms* (Version 2.21.0; Bürkner, 2017, 2018, 2021), *citr* (Version 0.3.2; Aust, 2019), *cmdstanr* (Version 0.8.1.9000; Gabry, Češnovar, Johnson, & Broder, 2024), *dplyr* (Version 1.1.4; Wickham, François, Henry, Müller, & Vaughan, 2023), *forcats* (Version 1.0.0; Wickham, 2023a), *ggplot2* (Version 3.5.1; Wickham, 2016), *lme4* (Version 1.1.35.5; Bates, Mächler, Bolker, & Walker, 2015), *lubridate* (Version 1.9.3; Grolemund & Wickham, 2011), *Matrix* (Version 1.7.0; Bates, Maechler, & Jagan, 2024), *nlme* (Version 3.1.166; Pinheiro & Bates, 2000), *papaja* (Version 0.1.2.9000; Aust & Barth, 2023), *patchwork* (Version 1.2.0; Pedersen, 2024), *purrr* (Version 1.0.2; Wickham & Henry, 2023), *RColorBrewer* (Version 1.1.3; Neuwirth, 2022), *Rcpp* (Eddelbuettel & Balamuta, 2018; Version 1.0.12; Eddelbuettel & François, 2011), *readr* (Version 2.1.5; Wickham, Hester, & Bryan, 2024), *RJ-2021-048* (Bengtsson, 2021), *standist* (Version 0.0.0.9000; Girard, 2024), *stringr* (Version 1.5.1; Wickham, 2023b), *tibble* (Version 3.2.1; Müller & Wickham, 2023), *tidybayes* (Version 3.0.6; Kay, 2023), *tidyverse* (Version 2.0.0; Wickham et al., 2019), and *tinylabels* (Version 0.2.4; Barth, 2023).

304 custom functions).

305 Our list of tutorials is as follows:

- 306 • 1a. Wrangle raw data and calculate descriptive stats for one independent variable
- 307 • 1b. Wrangle raw data and calculate descriptive stats for two independent variables
- 308 • 2a. Bayesian multilevel modeling for  $h(t)$
- 309 • 2b. Bayesian multilevel modeling for  $ca(t)$
- 310 • 3a. Frequentist multilevel modeling for  $h(t)$
- 311 • 3b. Frequentist multilevel modeling for  $ca(t)$
- 312 • 4. Simulation and power analysis for planning experiments

313 **4.1 Tutorial 1a: Calculating descriptive statistics using a life table**

314 **4.1.1 Data wrangling aims.** Our data wrangling procedures serve two related  
315 purposes. First, we want to summarise and visualise descriptive statistics that relate to our  
316 main research questions about the time course of psychological processes, using a life table.  
317 A life table includes for each time bin, the risk set (i.e., the number of trials that are  
318 event-free at the start of the bin), the number of observed events, and the estimates of  
319  $h(t)$ ,  $S(t)$ ,  $P(t)$ , possibly  $ca(t)$ , and their estimated standard errors (se).

320 Second, we want to produce two different data sets that can each be submitted to  
321 different types of inferential modelling approaches. The two types of data structure we  
322 label as ‘person-trial’ data and ‘person-trial-bin’ data. The ‘person-trial’ data (Table 1)  
323 will be familiar to most researchers who record behavioural responses from participants, as  
324 it represents the measured RT and accuracy per trial within an experiment. This data set  
325 is used when fitting conditional accuracy models (Tutorials 2b and 3b).

Table 1

*Data structure for ‘person-trial’ data*

pid	trial	condition	rt	accuracy
1	1	congruent	373.49	1
1	2	incongruent	431.31	1
1	3	congruent	455.43	0
1	4	incongruent	622.41	1
1	5	incongruent	535.98	1
1	6	incongruent	540.08	1
1	7	congruent	511.07	1
1	8	incongruent	444.42	1
1	9	congruent	678.69	1
1	10	congruent	549.79	1

*Note.* The first 10 trials for participant 1 are shown. These data are simulated and for illustrative purposes only.

326 In contrast, the ‘person-trial-bin’ data (Table 2) has a different, more extended  
 327 structure, which indicates in which bin a response occurred, if at all, in each trial.  
 328 Therefore, the ‘person-trial-bin’ data set generates a 0 in each bin until an event occurs  
 329 and then it generates a 1 to signal an event has occurred in that bin. This data set is used  
 330 when fitting hazard models (Tutorials 2a and 3a). It is worth pointing out that there is no  
 331 requirement for an event to occur at all (in any bin), as maybe there was no response on  
 332 that trial or the event occurred after the time window of interest. Likewise, when the event  
 333 occurs in bin 1 there would only be one row of data for that trial in the person-trial-bin  
 334 data set.

Table 2  
*Data structure for ‘person-trial-bin’ data*

pid	trial	condition	timebin	event
1	1	congruent	1	0
1	1	congruent	2	0
1	1	congruent	3	0
1	1	congruent	4	1
1	2	incongruent	1	0
1	2	incongruent	2	0
1	2	incongruent	3	0
1	2	incongruent	4	0
1	2	incongruent	5	1

*Note.* The first 2 trials for participant 1 from Table 1 are shown. The width of the time bins is 100 ms. These data are simulated and for illustrative purposes only.

335       **4.1.2 A real data wrangling example.** To illustrate how to quickly set up life  
 336 tables for calculating the descriptive statistics (functions of discrete time), we use a  
 337 published data set on masked response priming from Panis and Schmidt (2016). In their  
 338 first experiment, Panis and Schmidt (2016) presented a double arrow for 94 ms that  
 339 pointed left or right as the target stimulus with an onset at time point zero in each trial.  
 340 Participants had to indicate the direction in which the double arrow pointed using their  
 341 corresponding index finger, within 800 ms after target onset. Response time and accuracy  
 342 were recorded on each trial. Prime type (blank, congruent, incongruent) and mask type  
 343 were manipulated. Here we focus on the subset of trials in which no mask was presented.

344 The 13-ms prime stimulus was a double arrow presented 187 ms before target onset in the  
 345 congruent (same direction as target) and incongruent (opposite direction as target) prime  
 346 conditions.

347 There are several data wrangling steps to be taken. First, we need to load the data  
 348 before we (a) supply required column names, and (b) specify the factor condition with the  
 349 correct levels and labels.

350 The required column names are as follows:

- 351 • “pid”, indicating unique participant IDs;
- 352 • “trial”, indicating each unique trial per participant;
- 353 • “condition”, a factor indicating the levels of the independent variable (1, 2, ...) and  
   the corresponding labels;
- 355 • “rt”, indicating the response times in ms;
- 356 • “acc”, indicating the accuracies (1/0).

357 In the code of Tutorial 1a, this is accomplished as follows.

```
data_wr<-read_csv("../Tutorial_1_descriptive_stats/data/DataExp1_6subjects_wrangled.csv")
colnames(data_wr) <- c("pid","bl","tr","condition","resp","acc","rt","trial")
data_wr <- data_wr %>%
  mutate(condition = condition + 1, # original levels were 0, 1, 2.
        condition = factor(condition,
                             levels=c(1,2,3),
                             labels=c("blank","congruent","incongruent")))
```

358 Next, we can set up the life tables and plots of the discrete-time functions  $h(t)$ ,  $S(t)$ ,  
 359  $ca(t)$ , and  $P(t)$  – see part A of the supplementary material for their definitions. To do so  
 360 using a functional programming approach, one has to nest the data within participants  
 361 using the `group_nest()` function, and supply a user-defined censoring time and bin width  
 362 to our custom function “`censor()`”, as follows.

```

data_nested <- data_wr %>% group_nest(pid)

data_final <- data_nested %>%
  # ! user input: censoring time, and bin width
  mutate(censored = map(data, censor, 600, 40)) %>%
  # create person-trial-bin data set
  mutate(ptb_data = map(censored, ptb)) %>%
  # create life tables without ca(t)
  mutate(lifetable = map(ptb_data, setup_lt)) %>%
  # calculate ca(t)
  mutate(condacc = map(censored, calc_ca)) %>%
  # create life tables with ca(t)
  mutate(lifetable_ca = map2(lifetable, condacc, join_lt_ca)) %>%
  # create plots
  mutate(plot = map2(.x = lifetable_ca, .y = pid, plot_eha,1))

```

363 Note that the censoring time should be a multiple of the bin width (both in ms). The

364 censoring time should be a time point after which no informative responses are expected

365 anymore. In experiments that implement a response deadline in each trial the censoring

366 time can equal that deadline time point. Trials with a RT larger than the censoring time,

367 or trials in which no response is emitted during the data collection period, are treated as

368 right-censored observations in EHA. In other words, these trials are not discarded, because

369 they contain the information that the event did not occur before the censoring time.

370 Removing such trials before calculating the mean event time will result in underestimation

371 of the true mean.

372 The person-trial-bin oriented data set is created by our custom function ptb(), and it

373 has one row for each time bin (of each trial) that is at risk for event occurrence. The

374 variable “event” in the person-trial-bin oriented data set indicates whether a response

375 occurs (1) or not (0) for each bin.

376 The next step is to set up the life table using our custom function setup\_lt(),

377 calculate the conditional accuracies using our custom function `calc_ca()`, add the `ca(t)`  
378 estimates to the life table using our custom function `join_lt_ca()`, and then plot the  
379 descriptive statistics using our custom function `plot_eha()`. When creating the plots, some  
380 warning messages will likely be generated, like these:

- 381 • Removed 2 rows containing missing values or values outside the scale range  
382     (`geom_line()`).  
383 • Removed 2 rows containing missing values or values outside the scale range  
384     (`geom_point()`).  
385 • Removed 2 rows containing missing values or values outside the scale range  
386     (`geom_segment()`).

387 The warning messages are generated because some bins have no hazard and `ca(t)`  
388 estimates, and no error bars. They can thus safely be ignored. One can now inspect  
389 different aspects, including the life table for a particular condition of a particular subject,  
390 and a plot of the different functions for a particular participant. In general, it is important  
391 to visually inspect the functions first for each participant, in order to identify individuals  
392 that may be guessing (e.g., a flat conditional accuracy function at .5 indicates that  
393 someone is just guessing), outlying individuals, and/or different groups with qualitatively  
394 different behavior.

395 Table 3 shows the life table for condition “blank” (no prime stimulus presented) for  
396 participant 6. At time point zero, no events can occur and therefore  $h(t=0)$  and  $ca(t=0)$   
397 are undefined.

Table 3

*The life table for the blank prime condition of participant 6.*

bin	risk_set	events	hazard	se_haz	survival	se_surv	ca	se_ca
0	220	NA	NA	NA	1.00	0.00	NA	NA
40	220	0	0.00	0.00	1.00	0.00	NA	NA
80	220	0	0.00	0.00	1.00	0.00	NA	NA
120	220	0	0.00	0.00	1.00	0.00	NA	NA
160	220	0	0.00	0.00	1.00	0.00	NA	NA
200	220	0	0.00	0.00	1.00	0.00	NA	NA
240	220	0	0.00	0.00	1.00	0.00	NA	NA
280	220	7	0.03	0.01	0.97	0.01	0.29	0.17
320	213	13	0.06	0.02	0.91	0.02	0.77	0.12
360	200	26	0.13	0.02	0.79	0.03	0.92	0.05
400	174	40	0.23	0.03	0.61	0.03	1.00	0.00
440	134	48	0.36	0.04	0.39	0.03	0.98	0.02
480	86	37	0.43	0.05	0.22	0.03	1.00	0.00
520	49	32	0.65	0.07	0.08	0.02	1.00	0.00
560	17	9	0.53	0.12	0.04	0.01	1.00	0.00
600	8	4	0.50	0.18	0.02	0.01	1.00	0.00

*Note.* The column named “bin” indicates the endpoint of each time bin (in ms), and includes time point zero. For example the first bin is (0,40] with the starting point excluded and the endpoint included. At time point zero, no events can occur and therefore  $h(t=0)$  and  $ca(t=0)$  are undefined.  $se =$  standard error.  $ca =$  conditional accuracy.

Figure 4 displays the discrete-time hazard, survivor, conditional accuracy, and

399 probability mass functions for each prime condition for participant 6. By using  
 400 discrete-time hazard functions of event occurrence – in combination with conditional  
 401 accuracy functions for two-choice tasks – one can provide an unbiased, time-varying, and  
 402 probabilistic description of the latency and accuracy of responses based on all trials of any  
 403 data set.

## Descriptive stats for subject 6

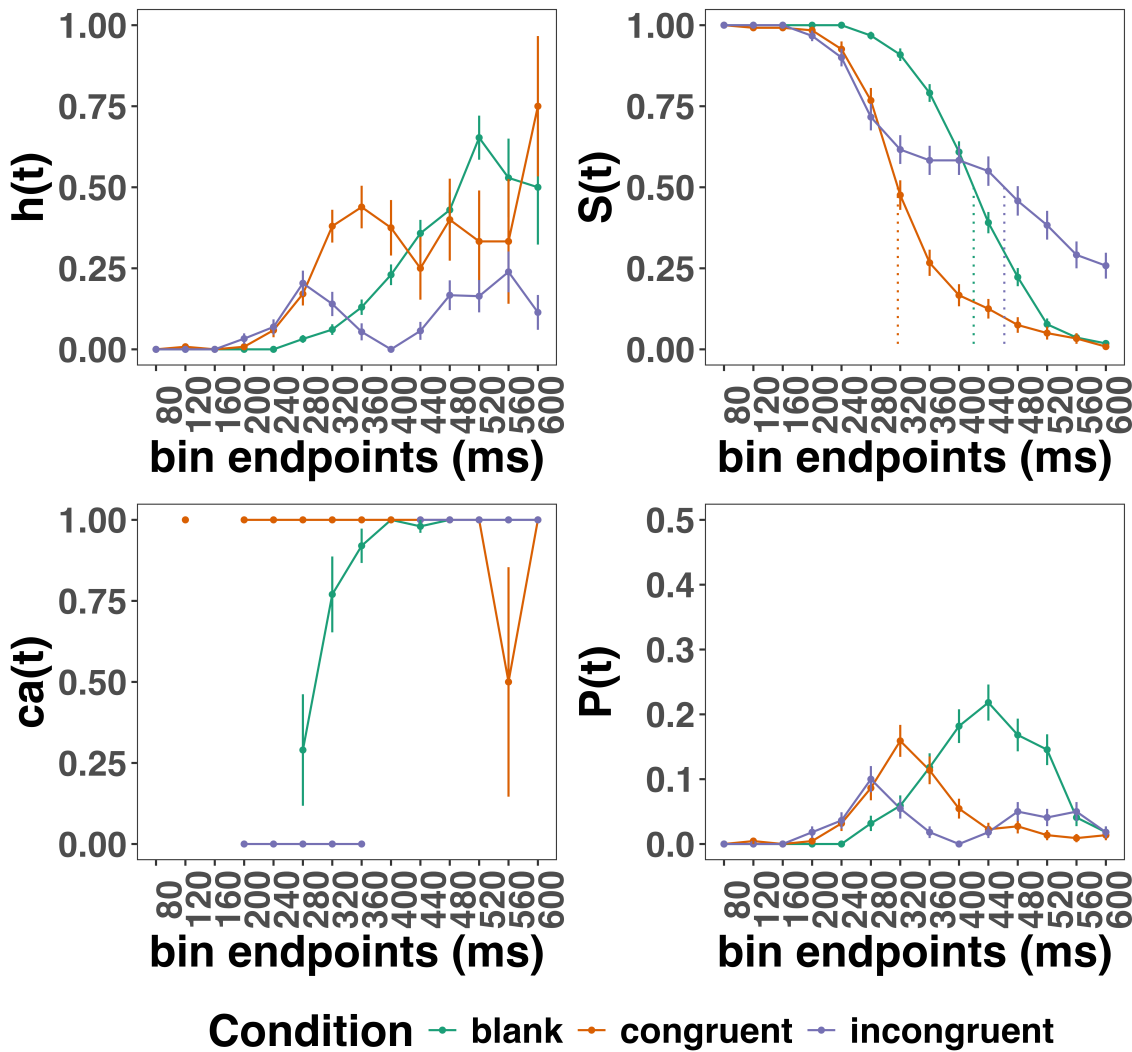


Figure 4. Estimated discrete-time hazard, survivor, probability mass, and conditional accuracy functions for participant 6. Vertical dotted lines indicate the estimated median RTs. Error bars represent 95% confidence intervals for the respective proportion.

404 For example, for participant 6, the estimated hazard values in bin (240,280] are 0.03,

405 0.17, and 0.20 for the blank, congruent, and incongruent prime conditions, respectively. In

406 other words, when the waiting time has increased until *240 ms* after target onset, then the

407 conditional probability of response occurrence in the next 40 ms is more than five times

408 larger for both prime-present conditions, compared to the blank prime condition.

409 Furthermore, the estimated conditional accuracy values in bin (240,280] are 0.29, 1,

410 and 0 for the blank, congruent, and incongruent prime conditions, respectively. In other

411 words, if a response is emitted in bin (240,280], then the probability that it is correct is

412 estimated to be 0.29, 1, and 0 for the blank, congruent, and incongruent prime conditions,

413 respectively.

414 However, when the waiting time has increased until *400 ms* after target onset, then

415 the conditional probability of response occurrence in the next 40 ms is estimated to be

416 0.36, 0.25, and 0.06 for the blank, congruent, and incongruent prime conditions,

417 respectively. And when a response does occur in bin (400,440], then the probability that it

418 is correct is estimated to be 0.98, 1, and 1 for the blank, congruent, and incongruent prime

419 conditions, respectively.

420 These distributional results suggest that the participant 6 is initially responding to

421 the prime even though (s)he was instructed to only respond to the target, that response

422 competition emerges in the incongruent prime condition around 300 ms, and that only

423 slower responses are fully controlled by the target stimulus. Qualitatively similar results

424 were obtained for the other five participants. When participants show qualitatively the

425 same distributional patterns, one might consider to aggregate their data and make one plot

426 (see Tutorial\_1a.Rmd).

427 In general, these results go against the (often implicit) assumption in research on

428 priming that all observed responses are primed responses to the target stimulus. Instead,

429 the distributional data show that early responses are triggered exclusively by the prime

430 stimulus, while only later responses reflect primed responses to the target stimulus.

431 At this point, we have calculated, summarised and plotted descriptive statistics for  
432 the key variables in EHA/SAT. As we will show in later Tutorials, statistical models for  
433  $h(t)$  and  $ca(t)$  can be implemented as generalized linear mixed regression models predicting  
434 event occurrence (1/0) and conditional accuracy (1/0) in each bin of a selected time  
435 window for analysis. But first we consider calculating the descriptive statistics for two  
436 independent variables.

#### 437 **4.2 Tutorial 1b: Generalising to a more complex design**

438 So far in this paper, we have used a simple experimental design, which involved one  
439 condition with three levels. But psychological experiments are often more complex, with  
440 crossed factorial designs with more conditions and more than three levels. The purpose of  
441 Tutorial 1b, therefore, is to provide a generalisation of the basic approach, which extends  
442 to a more complicated design. We felt that this might be useful for researchers in  
443 experimental psychology that typically use crossed factorial designs.

444 To this end, Tutorial 1b illustrates how to calculate and plot the descriptive statistics  
445 for the full data set of Experiment 1 of Panis and Schmidt (2016), which includes two  
446 independent variables: mask type and prime type. As we use the same functional  
447 programming approach as in Tutorial 1a, we simply present the sample-based functions for  
448 each participant as part of Tutorial 1b for those that are interested.

#### 449 **4.3 Tutorial 2a: Fitting Bayesian hazard models to discrete time-to-event data**

450 In this third tutorial, we illustrate how to fit Bayesian multi-level regression models  
451 to the RT data of the masked response priming data set used in Tutorial 1a. Fitting  
452 (Bayesian or non-Bayesian) regression models to time-to-event data is important when you  
453 want to study how the shape of the hazard function depends on various predictors (Singer

454 & Willett, 2003).

455 **4.3.1 Hazard model considerations.** There are several analytic decisions one has  
456 to make when fitting a discrete-time hazard model. First, one has to select an analysis time  
457 window, i.e., a contiguous set of bins for which there is enough data for each participant.  
458 Second, given that the dependent variable (event occurrence) is binary, one has to select a  
459 link function (see part C in the supplementary material). The cloglog link is preferred over  
460 the logit link when events can occur in principle at any time point within a bin, which is  
461 the case for RT data (Singer & Willett, 2003). Third, one has to choose whether to treat  
462 TIME (i.e., the time bin index  $t$ ) as a discrete or continuous predictor. And when you treat  
463 time as a discrete predictor, you can choose between reference coding and index coding.

464 In the case of a large- $N$  design without repeated measurements, the parameters of a  
465 discrete-time hazard model can be estimated using standard logistic regression software  
466 after expanding the typical person-trial data set into a person-trial-bin data set (Allison,  
467 2010). When there is clustering in the data, as in the case of a small- $N$  design with  
468 repeated measurements, the parameters of a discrete-time hazard model can be estimated  
469 using population-averaged methods (e.g., Generalized Estimating Equations), and Bayesian  
470 or frequentist generalized linear mixed models (Allison, 2010).

471 In general, there are three assumptions one can make or relax when adding  
472 experimental predictor variables and other covariates: The linearity assumption for  
473 continuous predictors (the effect of a 1 unit change is the same anywhere on the scale), the  
474 additivity assumption (predictors do not interact), and the proportionality assumption  
475 (predictors do not interact with TIME).

476 In tutorial\_2a.Rmd we fit several Bayesian multilevel models (i.e., generalized linear  
477 mixed models) that differ in complexity to the person-trial-bin oriented data set that we  
478 created in Tutorial 1a. We decided to select the analysis time window (200,600] and the  
479 cloglog link. Below, we shortly discuss three of these models. The person-trial-bin data set  
480 is prepared as follows.

```
# read in the file we saved in tutorial 1a
ptb_data <- read_csv("Tutorial_1_descriptive_stats/data/inputfile_hazard_modeling.csv")

ptb_data <- ptb_data %>%
  # select analysis time range: (200,600] with 10 bins (time bin ranks 6 to 15)
  filter(period > 5) %>%
    # continuous predictor for TIME named "period_9", centered on bin 9
  mutate(period_9 = period - 9,
        # categorical predictor for TIME named "timebin" with index coding
        timebin = factor(period,levels=c(6:15)),
        # factor "condition" using reference coding, with "blank" as the reference level
        condition = factor(condition, labels = c("blank", "congruent","incongruent")),
        # categorical predictor "prime" with index coding
        prime = ifelse(condition=="blank",1, ifelse(condition=="congruent",2,3)),
        prime = factor(prime,levels=c(1,2,3)))
```

481       **4.3.2 Prior distributions.** To get the posterior distribution of each model

482 parameter given the data, we need to specify prior distributions for the model parameters  
 483 which reflect our prior beliefs. In Tutorial\_2a.Rmd we perform some prior predictive  
 484 checks to make sure our selected prior distributions reflect our prior beliefs.

485       The middle column of Figure 16 in part E of the supplementary material shows six  
 486 examples of prior distributions for an intercept on the logit and/or cloglog scales. While a  
 487 normal distribution with relatively large variance is often used as a weakly informative  
 488 prior for continuous dependent variables, rows A and B in supplementary Figure 16 show  
 489 that specifying such distributions on the logit and cloglog scales actually leads to rather  
 490 informative distributions on the original probability scale, as most mass is pushed to  
 491 probabilities of 0 and 1.

492       **4.3.3 Model M0i: A null model with index coding.** When you do not want to  
 493 make assumptions about the shape of the hazard function, or its shape is not smooth but

494 irregular, then you can use a general specification of TIME, i.e., fit one grand intercept per  
 495 time bin. In this first model, we use a general specification of TIME using index coding,  
 496 and do not include experimental predictors. We call this model “M0i”.

497 Before we fit model M0i, we select the necessary columns from the data, and specify  
 498 our priors. In the code of Tutorial 2a, model M0i is specified as follows.

```
model_M0i <-
  brm(data = data_M0i,
       family = bernoulli(link="cloglog"),
       formula = event ~ 0 + timebin + (0 + timebin | pid),
       prior = priors_M0i,
       chains = 4, cores = 4,
       iter = 3000, warmup = 1000,
       control = list(adapt_delta = 0.999,
                      step_size = 0.04,
                      max_treedepth = 12),
       seed = 12, init = "0",
       file = "Tutorial_2_Bayesian/models/model_M0i")
```

499 After selecting the bernoulli family and the cloglog link, the model formula is  
 500 specified. The specification “0 + …” removes the default intercept in brm(). The fixed  
 501 effects include an intercept for each level of timebin. Each of these intercepts is allowed to  
 502 vary across individuals (variable pid). Estimating model M0i took about 30 minutes on a  
 503 MacBook Pro (Sonoma 14.6.1 OS, 18GB Memory, M3 Pro Chip).

504 **4.3.4 Model M1i: Adding the effects of prime-target congruency.** Previous  
 505 research has shown that psychological effects typically change over time (Panis, 2020;  
 506 Panis, Moran, et al., 2020; Panis & Schmidt, 2022; Panis et al., 2017; Panis & Wagemans,  
 507 2009). In the next model, we use index coding for both TIME (variable “timebin”) and the

508 categorical predictor prime-target-congruency (variable “prime”), so that we get 30 grand  
 509 intercepts, one for each combination of timebin level and prime level. Here is the model  
 510 formula of this model that we call “M1i”.

```
event ~ 0 + timebin:prime + (0 + timebin:prime | pid)
```

511 Estimating model M1i took about 124 minutes.

512 **4.3.4 Model M1d: A more parsimonious model.** When the shape of the  
 513 hazard function is rather smooth, as it is for behavioral RT data, one can fit a more  
 514 parsimonious model by treating TIME as a continuous variable, and use a polynomial  
 515 specification of the effect of TIME. Thus, if we want to make assumptions about (1) how  
 516 hazard changes over TIME in the reference condition (blank prime), and (2) how the effect  
 517 of congruent and incongruent primes change over TIME (relax the proportionality  
 518 assumption), then we can switch to a dummy coding approach for prime-target congruency  
 519 (variable “condition”) and treat TIME as a continuous variable (variable “period\_9”).

520 For example, we may assume that hazard can change in a linear + quadratic fashion  
 521 over time for a blank prime, and that the effects of congruent and incongruent primes  
 522 relative to blank change in a linear + quadratic fashion, and fit the model called “M1d”.  
 523 Here is its model formula.

```
event ~ 0 + Intercept + condition*period_9 + condition*period_9_sq +  

  (1 + condition*period_9 + condition*period_9_sq | pid)
```

524 The specification “0 + Intercept + . . . ” removes the default intercept in brm() and  
 525 adds an explicit Intercept for which we can set the prior ourselves. The variable  
 526 period\_9\_sq is a squared version of period\_9. Note that duplicate terms in the model  
 527 formula (e.g., condition) are ignored. Because TIME is centered on bin 9, the Intercept  
 528 represents the estimated cloglog-hazard in bin 9 for the blank prime condition. Model M1d  
 529 took about 145 minutes to run.

530        **4.3.5 Compare the models.** We can compare the three models using the Widely

531        Applicable Information Criterion (WAIC) and Leave-One-Out (LOO) cross-validation, and  
 532        look at model weights for both criteria (Kurz, 2023a; McElreath, 2018).

```
model_weights(model_M0i, model_M1i, model_M1d, weights = "loo") %>% round(digits = 2)
```

533 ## model\_M0i model\_M1i model\_M1d

534 ##            0            1            0

```
model_weights(model_M0i, model_M1i, model_M1d, weights = "waic") %>% round(digits = 2)
```

535 ## model\_M0i model\_M1i model\_M1d

536 ##            0            1            0

537        Clearly, both the loo and waic weighting schemes assign a weight of 1 to model M1i,

538        and a weight of 0 to the other two simpler models.

539        **4.3.6 Interpreting model M1i.** To make inferences from the parameter estimates

540        in model M1i, we first plot the densities of the draws from the posterior distributions of its

541        population-level parameters in Figure 5, together with point (median) and interval

542        estimates (80% and 95% credible intervals).

### Posterior distributions for population-level effects in Model M1i

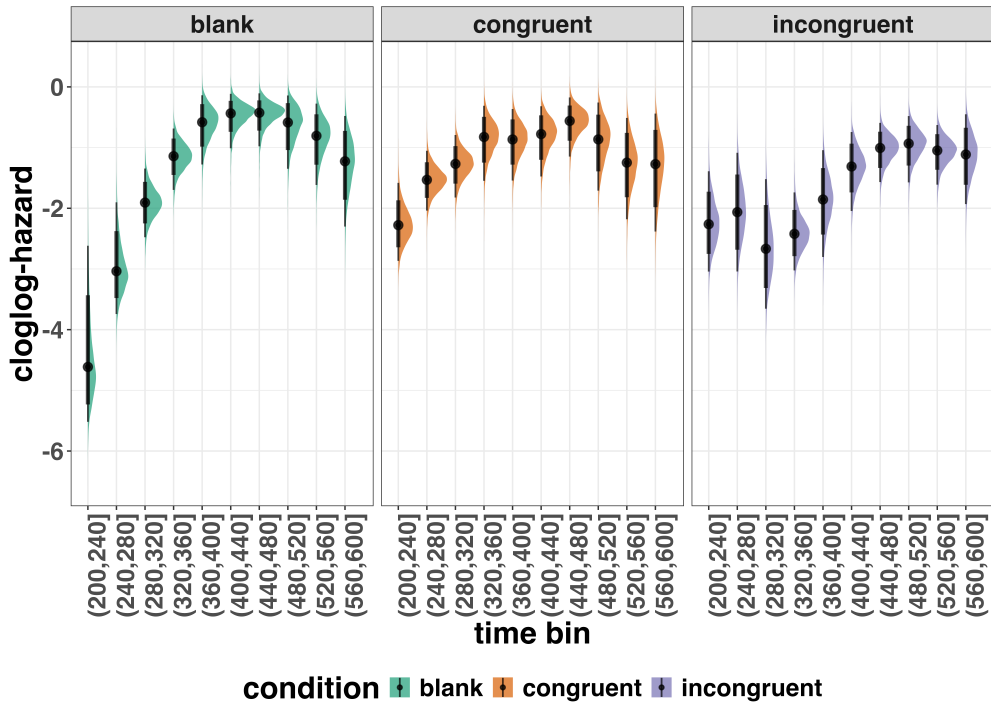


*Figure 5.* Medians and 80/95% credible intervals of the posterior distributions of the population-level parameters of model M1i.

Because the parameter estimates are on the cloglog-hazard scale, we can ease our

interpretation by plotting the expected value of the posterior predictive distribution – the predicted hazard values – for the average participant (Figure 6), and for each participant in the data set (Figure 7).

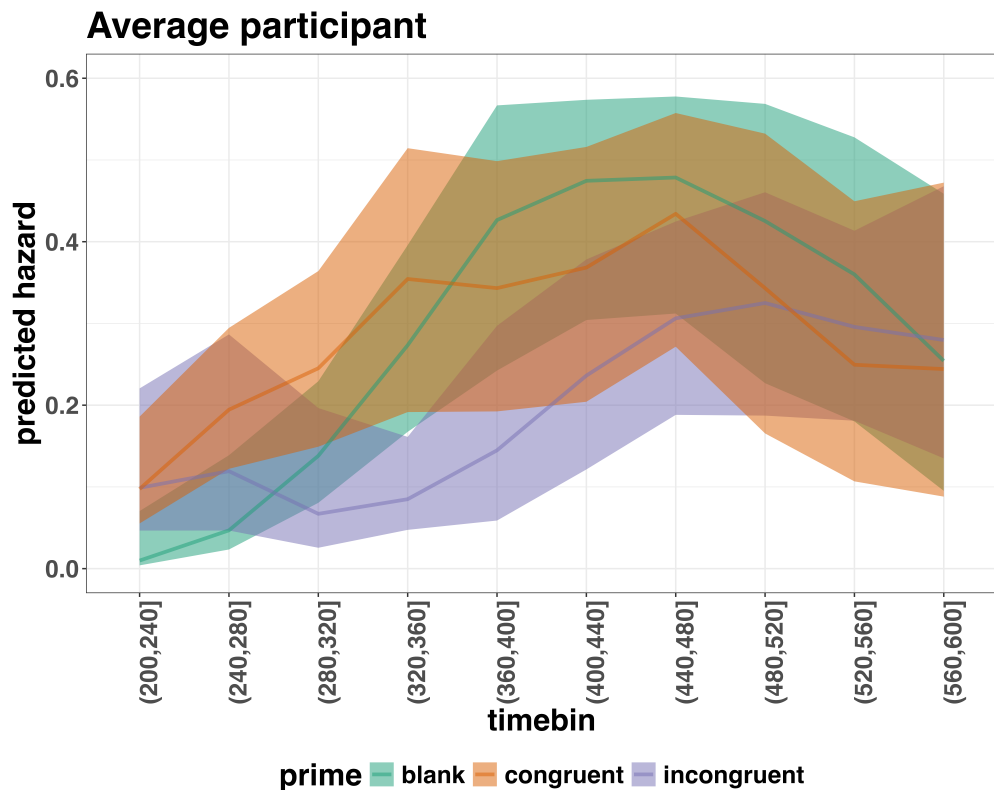


*Figure 6.* Point (median) and 80/95% credible interval summaries of the hazard estimates (expected values of the draws from the posterior predictive distributions) in each time bin for the average participant.

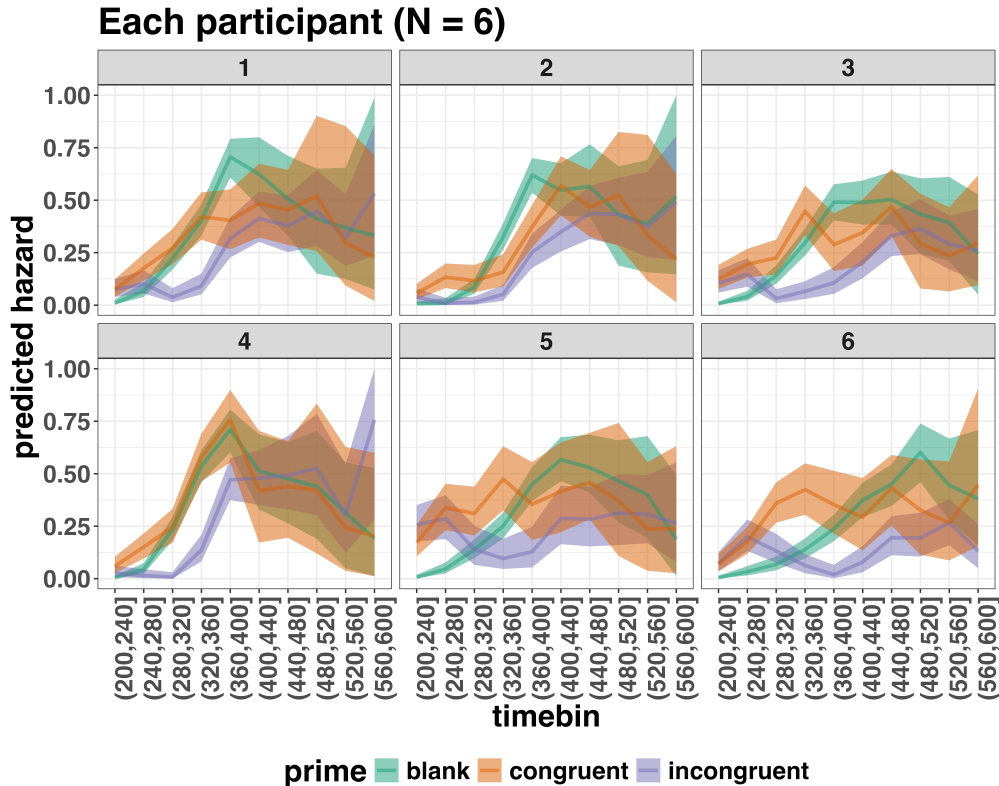


*Figure 7.* Point (median) and 80/95% credible interval summaries of the hazard estimates (expected values of the draws from the posterior predictive distributions) in each time bin for each participant.

547 As we are actually interested in the effects of congruent and incongruent primes,

548 relative to the blank prime condition, we can construct two contrasts (congruent-blank,  
 549 incongruent-blank), and plot the posterior distributions of these contrast effects, both for  
 550 the average participant (Figure 8; grand average marginal effect) and for each participant  
 551 in the data set (Figure 9; subject-specific average marginal effect).

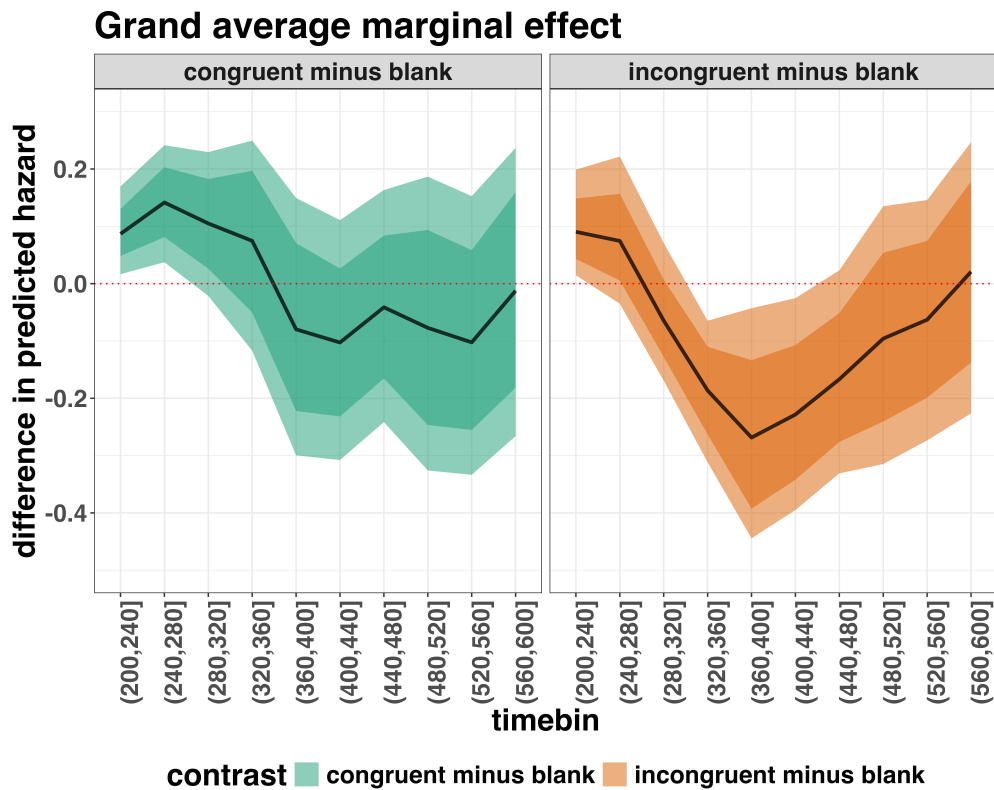


*Figure 8.* Point (mean) and 80/95% credible interval summaries of estimated differences in hazard in each time bin for the average participant.

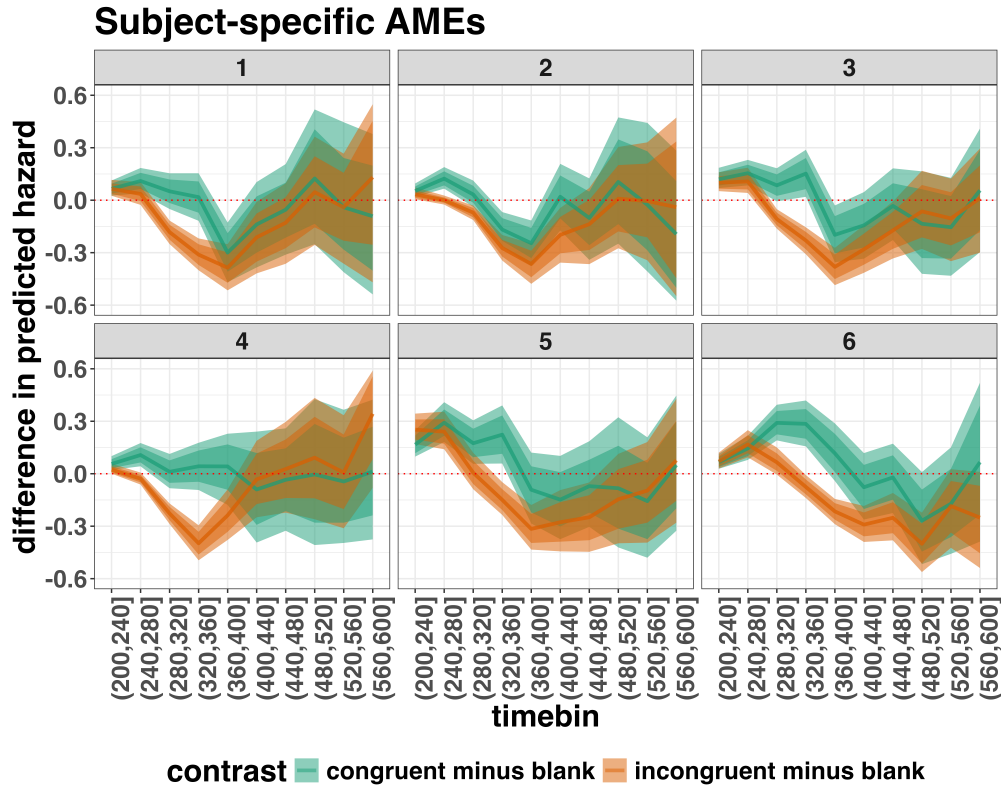


Figure 9. Point (mean) and 80/95% credible interval summaries of estimated differences in hazard in each time bin for each participant.

Table 4 shows the summaries of the estimated hazard differences for both contrasts in terms of a point estimate (the mean) and the upper and lower bounds of the 95% credible interval, for the average participant.

Table 4

*Point (mean) and 95% credible interval summary of estimated differences in hazard, for each time bin and contrast, in the average participant.*

contrast	timebin	diff	.lower	.upper
congruent minus blank	6	0.09	0.02	0.17

Table 4 continued

contrast	timebin	diff	.lower	.upper
congruent minus blank	7	0.14	0.04	0.25
congruent minus blank	8	0.11	-0.02	0.24
congruent minus blank	9	0.08	-0.12	0.27
congruent minus blank	10	-0.08	-0.30	0.15
congruent minus blank	11	-0.10	-0.31	0.11
congruent minus blank	12	-0.04	-0.24	0.17
congruent minus blank	13	-0.08	-0.33	0.20
congruent minus blank	14	-0.10	-0.33	0.15
congruent minus blank	15	-0.01	-0.27	0.27
incongruent minus blank	6	0.09	0.01	0.21
incongruent minus blank	7	0.08	-0.03	0.23
incongruent minus blank	8	-0.06	-0.17	0.07
incongruent minus blank	9	-0.19	-0.31	-0.06
incongruent minus blank	10	-0.27	-0.45	-0.04
incongruent minus blank	11	-0.23	-0.40	-0.03
incongruent minus blank	12	-0.17	-0.33	0.02
incongruent minus blank	13	-0.10	-0.31	0.14
incongruent minus blank	14	-0.06	-0.27	0.15
incongruent minus blank	15	0.03	-0.23	0.27

*Note.* diff = difference in predicted hazard.

556        ***Example conclusions for M1i.*** What can we conclude from model M1i about

557        our research question, i.e., the temporal dynamics of the effect of prime-target congruency  
558        on RT? In other words, in which of the 40-ms time bins between 200 and 600 ms after  
559        target onset does changing the prime from blank to congruent or incongruent affect the  
560        hazard of response occurrence (for a prime-target SOA of 187 ms)?

561        If we want to study the average effect of prime type on hazard, uncontaminated by

562        inter-individual differences, we can base our conclusion on Figure 8 and Table 4. The  
563        contrast “congruent minus blank” was estimated to be 0.09 hazard units in bin 6 (95% CrI  
564        = [0.02, 0.17]), and 0.14 hazard units in bin 7 (95% CrI = [0.04, 0.25]). For the other bins,  
565        the 95% credible interval contained zero. The contrast “incongruent minus blank” was  
566        estimated to be 0.09 hazard units in bin 6 (95% CrI = [0.01, 0.21]), -0.19 hazard units in  
567        bin 9 (95% CrI = [-0.31, -0.06]), -0.27 hazard units in bin 10 (95% CrI = [-0.45, -0.04]),  
568        and -0.23 hazard units in bin 11 (95% CrI = [-0.40, -0.03]). For the other bins, the 95%  
569        credible interval contained zero. Note that we could also have calculated hazard ratios  
570        instead of hazard differences.

571        There are thus two phases of performance for the average person between 200 and

572        600 ms after target onset. In the first phase, the addition of a congruent or incongruent  
573        prime stimulus increases the hazard of response occurrence compared to blank prime trials  
574        in the time period (200, 240]. In the second phase, only the incongruent prime decreases  
575        the hazard of response occurrence compared to blank primes, in the time period (320,440].  
576        The sign of the effect of incongruent primes on the hazard of response occurrence thus  
577        depends on how much waiting time has passed since target onset.

578        The posterior distribution of each contrast can also be summarized by considering its

579        proportion below or above some value, like zero. Table 5 shows the proportion of the  
580        posterior distribution below or above zero, for each time bin and contrast.

Table 5

*Summarizing the posterior distributions of each contrast by their proportion below and above zero.*

timebin	contrast	prop_above	prop_below
6	congruent minus blank	0.99	0.01
7	congruent minus blank	0.99	0.01
8	congruent minus blank	0.95	0.05
9	congruent minus blank	0.79	0.21
10	congruent minus blank	0.24	0.76
11	congruent minus blank	0.15	0.85
12	congruent minus blank	0.33	0.67
13	congruent minus blank	0.28	0.72
14	congruent minus blank	0.19	0.81
15	congruent minus blank	0.47	0.53
6	incongruent minus blank	0.98	0.02
7	incongruent minus blank	0.92	0.08
8	incongruent minus blank	0.12	0.88
9	incongruent minus blank	0.00	1.00
10	incongruent minus blank	0.01	0.99
11	incongruent minus blank	0.02	0.98
12	incongruent minus blank	0.04	0.96
13	incongruent minus blank	0.20	0.80
14	incongruent minus blank	0.27	0.73
15	incongruent minus blank	0.58	0.42

*Note.* prop\_below = proportion below zero; prop\_above = proportion above zero.

581

582        Thus, the probability that the contrast “congruent minus blank” is larger than 0, is  
583        larger than .9 in bins 6 to 8. And the probability that the contrast “incongruent minus  
584        blank” is smaller than 0, is larger than .9 in bins 9 to 12.

585        If we want to focus more on inter-individual differences, we can study the  
586        subject-specific hazard functions in Figure 9. Note that three participants (1, 2, and 3)  
587        show a negative difference for the contrast “congruent minus incongruent” in bin (360,400]  
588        – subject 2 also in bin (320,360].

589        Future studies could (a) increase the number of participants to estimate the  
590        proportion of “dippers” in the subject population, and/or (b) try to explain why this dip  
591        occurs. For example, Panis and Schmidt (2016) concluded that active, top-down,  
592        task-guided response inhibition effects emerge around 360 ms after the onset of the  
593        stimulus following the prime (here: the target stimulus). Such a top-down inhibitory effect  
594        might exist in our priming data set, because after some time participants will learn that the  
595        first stimulus is not the one they have to respond to; To prevent a premature overt response  
596        to the prime they thus might gradually increase a global response threshold during the  
597        remainder of the experiment, which could result in a lower hazard in congruent trials  
598        compared to blank trials, for bins after ~360 ms, and towards the end of the experiment.  
599        This effect might be masked for incongruent primes by the response competition effect.

600        Interestingly, all subjects show a tendency in their mean difference (congruent minus  
601        blank) to “dip” around that time (Figure 9). Therefore, future modeling efforts could  
602        incorporate the trial number into the model formula, in order to also study how the effects  
603        of prime type on hazard change on the long experiment-wide time scale, next to the short  
604        trial-wide time scale. In Tutorial\_2a.Rmd we provide a number of model formula that  
605        should get you going.

606 **4.4 Tutorial 2b: Fitting Bayesian conditional accuracy models**

607 In this fourth tutorial, we illustrate how to fit a Bayesian multi-level regression model  
 608 to the timed accuracy data from the masked response priming data set used in Tutorial 1a.  
 609 The general process is similar to Tutorial 2a, except that (a) we use the person-trial data  
 610 set, (b) we use the logit link function, and (c) we change the priors. For illustration  
 611 purposes, we only fitted the effects of model M1i (see Tutorial 2a) in the conditional  
 612 accuracy model called M1i\_ca.

613 To make inferences from the parameter estimates in model M1i\_ca, we first plot the  
 614 densities of the draws from the posterior distributions of its population-level parameters in  
 615 Figure 10, together with point (median) and interval estimates (80% and 95% credible  
 616 intervals).

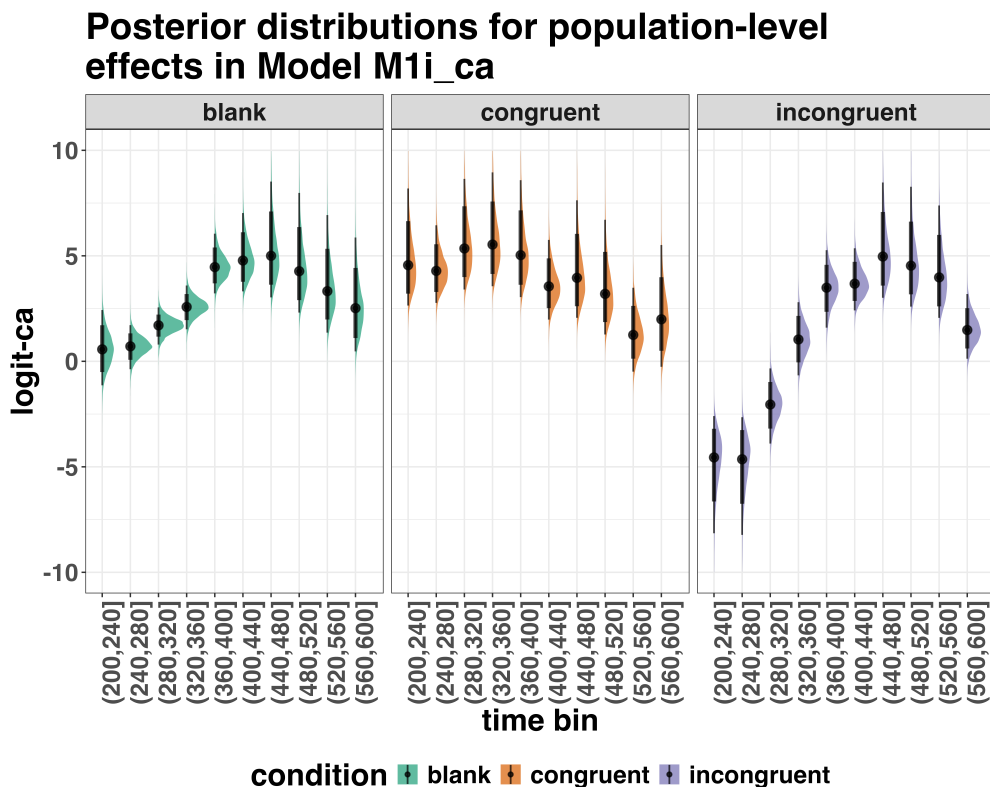


*Figure 10.* Medians and 80/95% credible intervals of the posterior distributions of the population-level parameters of model M1i\_ca.

Because the parameter estimates are on the logit-ca scale, we can ease our interpretation by plotting the expected value of the posterior predictive distribution – the predicted conditional accuracies – for the average participant (Figure 11), and for each participant in the data set (Figure 12).

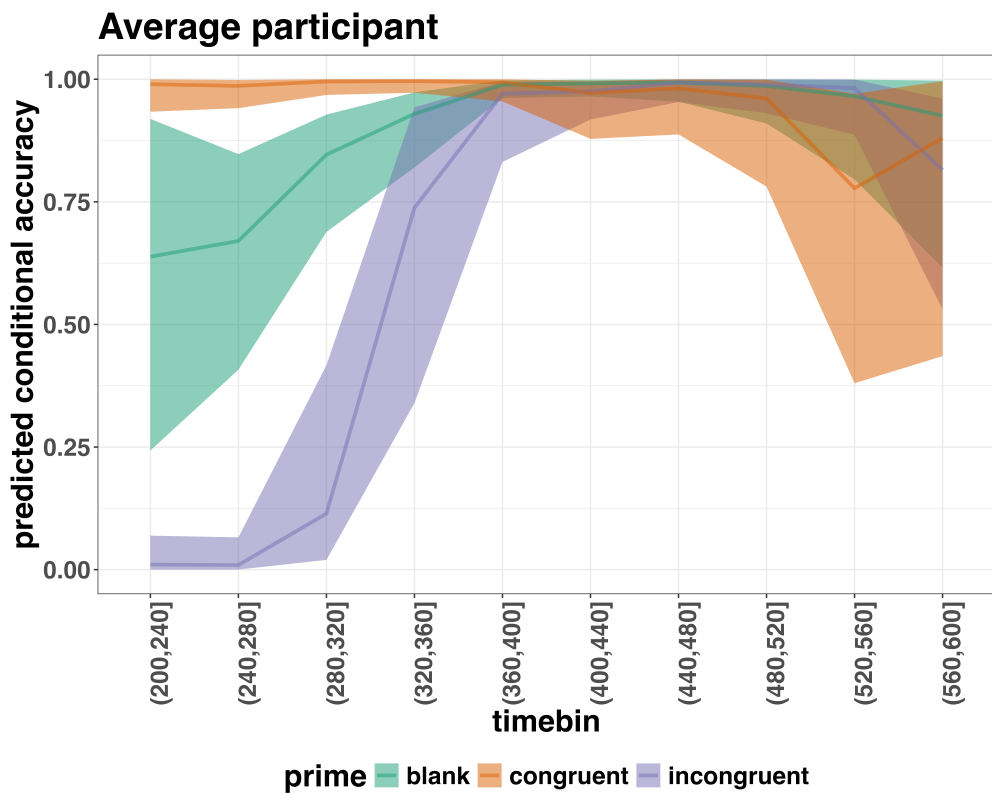
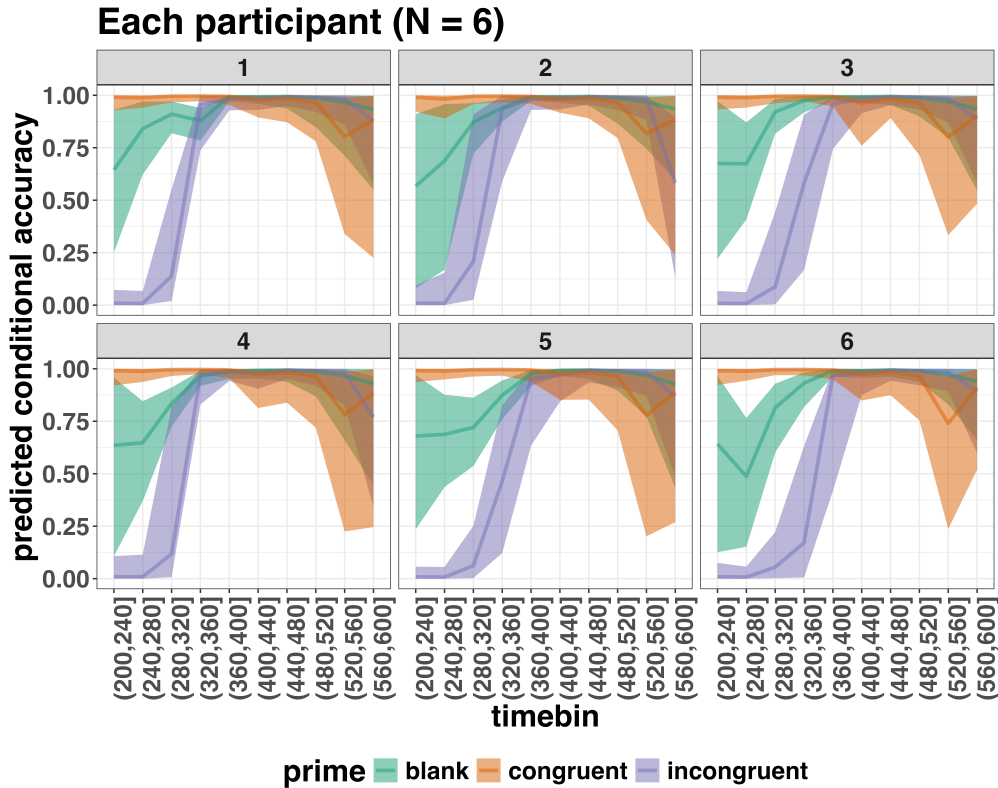


Figure 11. Point (median) and 80/95% credible interval summaries of the conditional accuracy estimates (expected values of the draws from the posterior predictive distributions) in each time bin for the average participant.



*Figure 12.* Point (median) and 80/95% credible interval summaries of the conditional accuracy estimates (expected values of the draws from the posterior predictive distributions) in each time bin for each participant.

As we are actually interested in the effects of congruent and incongruent primes,

relative to the blank prime condition, we can construct two contrasts (congruent-blank, incongruent-blank), and plot the posterior distributions of these contrast effects for the average participant (Figure 13; grand average marginal effect).

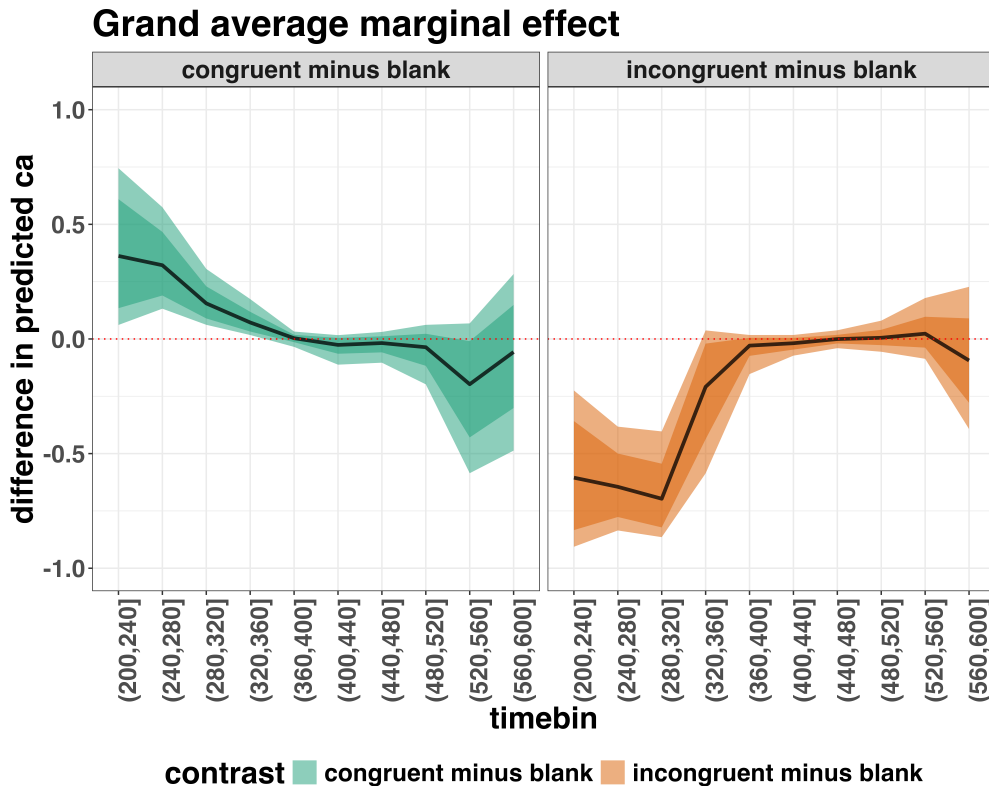


*Figure 13.* Point (mean) and 80/95% credible interval summaries of estimated differences in conditional accuracy in each time bin for the average participant.

625 Table 6 shows the summaries of the estimated differences in conditional accuracy for  
 626 both contrasts in terms of a point estimate (the mean) and the upper and lower bounds of  
 627 the 95% credible interval, for the average participant.

Table 6

*Point (mean) and 95% credible interval summary of estimated differences in conditional accuracy, for each time bin and contrast, in the average participant.*

contrast	timebin	diff_ca	.lower	.upper
congruent minus blank	6	0.36	0.06	0.74

Table 6 continued

contrast	timebin	diff_ca	.lower	.upper
congruent minus blank	7	0.32	0.13	0.57
congruent minus blank	8	0.16	0.06	0.31
congruent minus blank	9	0.07	0.02	0.17
congruent minus blank	10	0.00	-0.03	0.03
congruent minus blank	11	-0.03	-0.11	0.02
congruent minus blank	12	-0.02	-0.10	0.03
congruent minus blank	13	-0.04	-0.20	0.06
congruent minus blank	14	-0.20	-0.59	0.07
congruent minus blank	15	-0.06	-0.49	0.28
incongruent minus blank	6	-0.61	-0.91	-0.22
incongruent minus blank	7	-0.64	-0.84	-0.38
incongruent minus blank	8	-0.70	-0.86	-0.40
incongruent minus blank	9	-0.21	-0.59	0.04
incongruent minus blank	10	-0.03	-0.15	0.02
incongruent minus blank	11	-0.02	-0.07	0.02
incongruent minus blank	12	0.00	-0.04	0.04
incongruent minus blank	13	0.01	-0.06	0.08
incongruent minus blank	14	0.02	-0.09	0.18
incongruent minus blank	15	-0.09	-0.39	0.23

*Note.* diff = difference in predicted conditional accuracy.

630 on the conditional accuracy of emitted responses in time bins (200,240], (240,280], and  
631 (280,320], relative to the estimates in the baseline condition (blank prime; red dashed lines  
632 in Figure 14). Incongruent primes have a negative effect on the conditional accuracy of  
633 emitted responses in those time bins, relative to the estimates in the baseline condition.

634 **4.5 Tutorial 3a: Fitting Frequentist hazard models**

635 In this fifth tutorial we illustrate how to fit a multilevel regression model to RT data  
636 in the frequentist framework, for the data set used in Tutorial 1a. The general process is  
637 similar to that in Tutorial 2a, except that there are no priors to set.

638 For illustration purposes, we only fitted the effects from model M1i (see Tutorial 2a)  
639 using the function `glmer()` from the R package `lme4`. Alternatively, one could also use the  
640 function `glmmPQL()` from the R package `MASS` (Ripley et al., 2024). The resulting hazard  
641 model is called `M1i_f`.

642 In Figure 14 we compare the parameter estimates of model M1i from `brm()` with  
643 those of model `M1i_f` from `glmer()`.

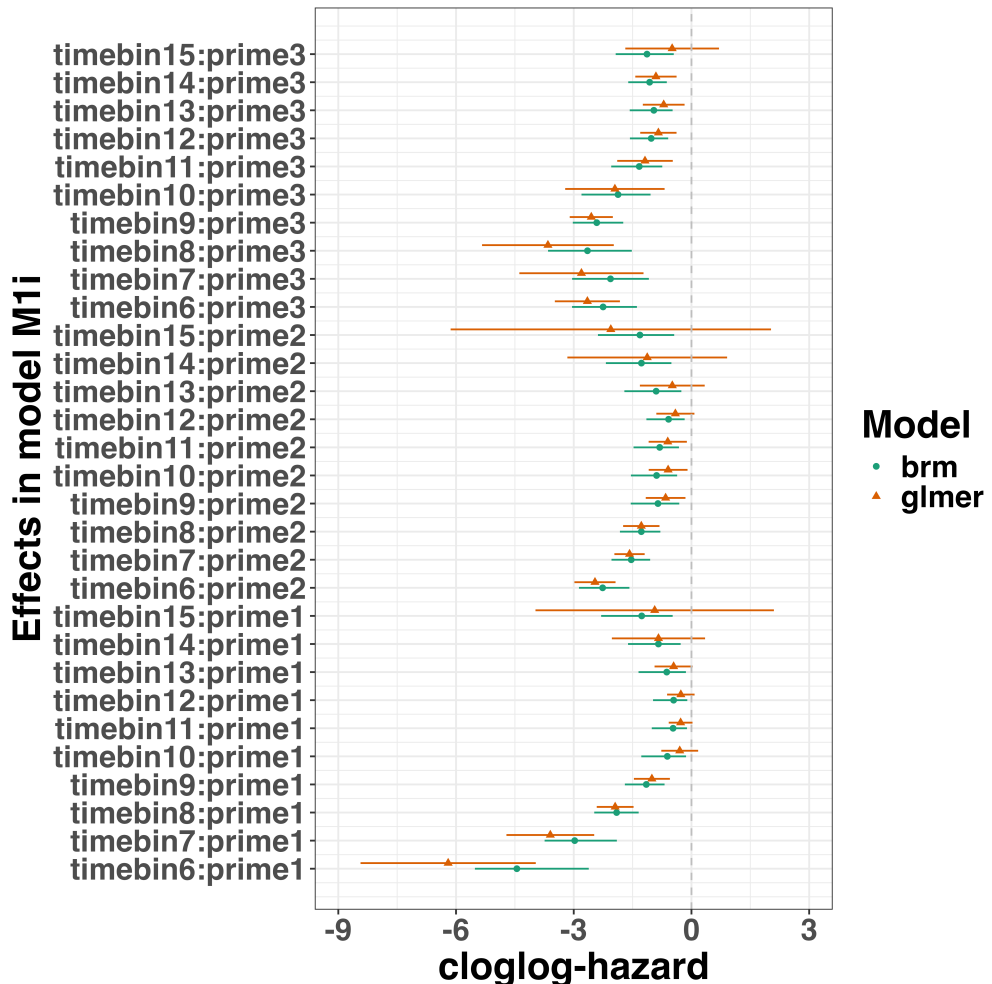


Figure 14. Parameter estimates for model M1i from `brm()` – means and 95% credible intervals – and model M1i\_f from `glmer()` – maximum likelihood estimates and 95% confidence intervals.

644 Figure 14 confirms that the parameter estimates from both Bayesian and frequentist

645 models are pretty similar, which makes sense given the close similarity in model structure.

646 However, model M1i\_f did not converge and resulted in a singular fit. This is of course one

647 of the reasons why Bayesian modeling has become so popular in recent years. But the price

648 you pay for being able to fit more complex random effects models in a Bayesian framework

649 is computation time. In other words, as we have noted throughout, some of the Bayesian

650 models in Tutorials 2a took several hours to build.

**651 4.6 Tutorial 3b: Fitting Frequentist conditional accuracy models**

652 In this sixth tutorial we illustrate how to fit a multilevel regression model to the  
653 timed accuracy data in the frequentist framework, for the data set used in Tutorial 1a. For  
654 illustration purposes, we only fitted the effects from model M1i\_ca (see Tutorial 2b) using  
655 the function glmer() from the R package lme4. Alternatively, one could also use the  
656 function glmmPQL() from the R package MASS (Ripley et al., 2024). Again, the resulting  
657 conditional accuracy model M1i\_ca\_f did not converge and resulted in a singular fit.

**658 4.4 Tutorial 4: Planning**

659 This needs adding... RR to do this.

**660 5. Discussion**

661 This main motivation for writing this paper is the observation that EHA and SAT  
662 analysis remain under-used in psychological research. As a consequence, the field of  
663 psychological research is not taking full advantage of the many benefits EHA/SAT provides  
664 compared to more conventional analyses. By providing a freely available set of tutorials,  
665 which provide step-by-step guidelines and ready-to-use R code, we hope that researchers  
666 will feel more comfortable using EHA/SAT in the future. Indeed, we hope that our  
667 tutorials may help to overcome a barrier to entry with EHA/SAT, which is that such  
668 approaches require more analytical complexity compared to mean-average comparisons.  
669 While we have focused here on within-subject, factorial, small- $N$  designs, it is important to  
670 realize that EHA/SAT can be applied to other designs as well (large- $N$  designs with only  
671 one measurement per subject, between-subject designs, etc.). As such, the general workflow  
672 and associated code can be modified and applied more broadly to other contexts and  
673 research questions. In the following, we discuss issues relating to model complexity and

674 interpretability, individual differences, as well as limitations of the approach and future  
675 extensions.

676 **5.1 What are the main use-cases of EHA for understanding cognition and brain  
677 function?**

678 For those researchers, like ourselves, who are primarily interested in understanding  
679 human cognitive and brain systems, we consider two broadly-defined, main use-cases of  
680 EHA. First, as we hope to have made clear by this point, EHA is one way to investigating  
681 a “temporal states” approach to cognitive processes. EHA provides one way to uncover  
682 when cognitive states may start and stop, as well as what they may be tied to or interact  
683 with. Therefore, if your research questions concern **when** and **for how long** psychological  
684 states occur, our EHA tutorials could be useful tools for you to use.

685 Second, even if you are not primarily interested in studying the temporal states of  
686 cognition, EHA could still be a useful tool to consider using, in order to qualify inferences  
687 that are being made based on mean-average comparisons. Given that distinctly different  
688 inferences can be made from the same data based on whether one computes a  
689 mean-average across trials or a RT distribution of events (Figure 1), it may be important  
690 for researchers to supplement mean-average comparisons with EHA. One could envisage  
691 scenarios where the implicit assumption of an effect manifesting across all of the time bins  
692 measured would not be supported by EHA. Therefore, the conclusion of interest would not  
693 apply to all responses, but instead it would be restricted to certain aspects of time.

694 **5.2 Model complexity versus interpretability**

695 EHA can quickly become very complex when adding more than 1 time scale, due to  
696 the many possible higher-order interactions. For example, model M4 contains two time  
697 scales as covariates: the passage of time on the within-trial time scale, and the passage of

698 time on the across-trial (or within-experiment) time scale. However, when trials are  
699 presented in blocks, and blocks of trials within sessions, and when the experiment  
700 comprises three sessions, then four time scales can be defined (within-trial, within-block,  
701 within-session, and within-experiment). From a theoretical perspective, adding more than  
702 1 time scale – and their interactions – can be important to capture plasticity and other  
703 learning effects that may play out on such longer time scales, and that are probably present  
704 in each experiment in general. From a practical perspective, therefore, some choices need  
705 to be made to balance the amount of data that is being collected per participant, condition  
706 and across the varying timescales. As one example, if there are several timescales of  
707 relevance, then it might be prudent for interpretational purposes to limit the number of  
708 experimental predictor variables (conditions). This is of course where planning and data  
709 simulation efforts would be important to provide a guide to experimental design choices.

### 710 5.3 Individual differences

711 One important issue is that of possible individual differences in the overall location of  
712 the distribution, and the time course of psychological effects. For example, when you wait  
713 for a response of the participant on each trial, you allow the participant to have control  
714 over the trial duration, and some participants might respond only when they are confident  
715 that their emitted response will be correct. These issues can be avoided by introducing a  
716 (relatively short) response deadline in each trial, e.g., 600 ms for simple detection tasks,  
717 1000 ms for more difficult discrimination tasks, or 2 s for tasks requiring extended high-level  
718 processing. Because EHA can deal in a straightforward fashion with right-censored  
719 observations (i.e., trials without an observed response), introducing a response deadline is  
720 recommended when designing RT experiments. Furthermore, introducing a response  
721 deadline and asking participants to respond before the deadline as much as possible, will  
722 also lead to individual distributions that overlap in time, which is important when selecting  
723 a common analysis time window when fitting hazard and conditional accuracy models.

724        But even when using a response deadline, participants can differ qualitatively in the  
725    effects they display (see Panis, 2020). One way to deal with this is to describe and  
726    interpret the different patterns. Another way is to run a clustering algorithm on the  
727    individual hazard estimates across all conditions. The obtained dendrogram can then be  
728    used to identify a (hopefully big) cluster of participants that behave similarly, and to  
729    identify a (hopefully small) cluster of participants with different behavioral patterns. One  
730    might then exclude the smaller sub-group of participants before fitting a hazard model or  
731    consider the possibility that different cognitive processes may be at play during task  
732    performance across the different sub-groups.

733        Another approach to deal with individual differences is Bayesian prevalence (Ince,  
734    Paton, Kay, & Schyns, 2021), which is a from of Small-N approach (Smith & Little, 2018).  
735    This method looks at effects within each individual in the study and asks how likely it  
736    would be to see the same result if the experiment was repeated with a new person chosen  
737    from the wider population at random. This approach allows one to quantify how typical or  
738    uncommon an observed effect is in the population, and the uncertainty around this  
739    estimate.

#### 740    5.4 Limitations

741        Compared to the orthodox method – comparing mean-averages between conditions –  
742    the most important limitation of multi-level hazard and conditional accuracy modeling is  
743    that it might take a long time to estimate the parameters using Bayesian methods or the  
744    model might have to be simplified significantly to use frequentist methods.

745        Another issue is that you need a relatively large number of trials per condition to  
746    estimate the hazard function with high temporal resolution, which is required when testing  
747    predictions of process models of cognition. Indeed, in general, there is a trade-off between  
748    the number of trials per condition and the temporal resolution (i.e., bin width) of the

749 hazard function. Therefore, we recommend researchers to collect as many trials as possible  
750 per experimental condition, given the available resources and considering the participant  
751 experience (e.g., fatigue and boredom). For instance, if the maximum session length  
752 deemed reasonable is between 1 and 2 hours, what is the maximum number of trials per  
753 condition that you could reasonably collect? After consideration, it might be worth  
754 conducting multiple testing sessions per participant and/or reducing the number of  
755 experimental conditions. Finally, there is a user-friendly online tool for calculating  
756 statistical power as a function of the number of trials as well as the number of participants,  
757 and this might be worth consulting to guide the research design process (Baker et al., 2021).

758 We did not discuss continuous-time EHA, nor continuous-time SAT analysis. As  
759 indicated by Allison (2010), learning discrete-time EHA methods first will help in learning  
760 continuous-time methods. Given that RT is typically treated as a continuous variable, it is  
761 possible that continuous-time methods will ultimately prevail. However, they require much  
762 more data to estimate the continuous-time hazard (rate) function well. Thus, by trading a  
763 bit of temporal resolution for a lower number of trials, discrete-time methods seem ideal for  
764 dealing with typical psychological time-to-event data sets for which there are less than  
765 ~200 trials per condition per experiment.

766 **5.5 Extensions**

767 The hazard models in this tutorial assume that there is one event of interest. For RT  
768 data, this event constitutes a single transition between an “idle” state and a “responded”  
769 state. However, in certain situations, more than one event of interest might exist. For  
770 example, in a medical or health-related context, an individual might transition back and  
771 forth between a “healthy” state and a “depressed” state, before being absorbed into a final  
772 “death” state. When you have data on the timing of these transitions, one can apply  
773 multi-state hazard models, which generalize EHA to transitions between three or more  
774 states (Steele, Goldstein, & Browne, 2004). Also, the predictor variables in this tutorial are

775 time-invariant, i.e., their value did not change over the course of a trial. Thus, another  
776 extension is to include time-varying predictors, i.e., predictors whose value can change  
777 across the time bins within a trial (Allison, 2010). For example, when gaze position is  
778 tracked during a visual search trial, the gaze-target distance will vary during a trial when  
779 the eyes move around before a manual response is given; shorter gaze-target distances  
780 should be associated with a higher hazard of response occurrence. Note that the effect of a  
781 time-varying predictor (e.g., an occipital EEG signal) can itself vary over time.

782 **6. Conclusions**

783 Estimating the temporal distributions of RT and accuracy provide a rich source of  
784 information on the time course of cognitive processing, which have been largely  
785 undervalued in the history of experimental psychology and cognitive neuroscience.  
786 Statistically controlling for the passage of time during data analysis is equally important as  
787 experimental control during the design of an experiment, to better understand human  
788 behavior in experimental paradigms. We hope that by providing a set of hands-on,  
789 step-by-step tutorials, which come with custom-built and freely available code, researchers  
790 will feel more comfortable embracing EHA and investigating the temporal profile of  
791 cognitive states. On a broader level, we think that wider adoption of such approaches will  
792 have a meaningful impact on the inferences drawn from data, as well as the development of  
793 theories regarding the structure of cognition.

794

## References

- 795 Allison, P. D. (1982). Discrete-Time Methods for the Analysis of Event Histories.  
796       *Sociological Methodology*, 13, 61. <https://doi.org/10.2307/270718>
- 797 Allison, P. D. (2010). *Survival analysis using SAS: A practical guide* (2. ed). Cary, NC:  
798       SAS Press.
- 799 Aust, F. (2019). *Citr: 'RStudio' add-in to insert markdown citations*. Retrieved from  
800       <https://github.com/crsh/citr>
- 801 Aust, F., & Barth, M. (2023). *papaja: Prepare reproducible APA journal articles with R*  
802       *Markdown*. Retrieved from <https://github.com/crsh/papaja>
- 803 Aust, F., & Barth, M. (2024). *papaja: Prepare reproducible APA journal articles with R*  
804       *Markdown*. <https://doi.org/10.32614/CRAN.package.papaja>
- 805 Baker, D. H., Vilidaite, G., Lygo, F. A., Smith, A. K., Flack, T. R., Gouws, A. D., &  
806 Andrews, T. J. (2021). Power contours: Optimising sample size and precision in  
807 experimental psychology and human neuroscience. *Psychological Methods*, 26(3),  
808 295–314. <https://doi.org/10.1037/met0000337>
- 809 Barr, D. J., Levy, R., Scheepers, C., & Tily, H. J. (2013). Random effects structure for  
810 confirmatory hypothesis testing: Keep it maximal. *Journal of Memory and Language*,  
811 68(3), 10.1016/j.jml.2012.11.001. <https://doi.org/10.1016/j.jml.2012.11.001>
- 812 Barth, M. (2023). *tinylabes: Lightweight variable labels*. Retrieved from  
813       <https://cran.r-project.org/package=tinylabes>
- 814 Bates, D., Mächler, M., Bolker, B., & Walker, S. (2015). Fitting linear mixed-effects  
815 models using lme4. *Journal of Statistical Software*, 67(1), 1–48.  
816       <https://doi.org/10.18637/jss.v067.i01>
- 817 Bates, D., Maechler, M., & Jagan, M. (2024). *Matrix: Sparse and dense matrix classes and*  
818       *methods*. Retrieved from <https://CRAN.R-project.org/package=Matrix>
- 819 Bengtsson, H. (2021). A unifying framework for parallel and distributed processing in r  
820 using futures. *The R Journal*, 13(2), 208–227. <https://doi.org/10.32614/RJ-2021-048>

- 821 Blossfeld, H.-P., & Rohwer, G. (2002). *Techniques of event history modeling: New*  
822 *approaches to causal analysis, 2nd ed* (pp. x, 310). Mahwah, NJ, US: Lawrence  
823 Erlbaum Associates Publishers.
- 824 Box-Steffensmeier, J. M. (2004). Event history modeling: A guide for social scientists.  
825 Cambridge: University Press.
- 826 Bürkner, P.-C. (2017). brms: An R package for Bayesian multilevel models using Stan.  
827 *Journal of Statistical Software*, 80(1), 1–28. <https://doi.org/10.18637/jss.v080.i01>
- 828 Bürkner, P.-C. (2018). Advanced Bayesian multilevel modeling with the R package brms.  
829 *The R Journal*, 10(1), 395–411. <https://doi.org/10.32614/RJ-2018-017>
- 830 Bürkner, P.-C. (2021). Bayesian item response modeling in R with brms and Stan. *Journal*  
831 *of Statistical Software*, 100(5), 1–54. <https://doi.org/10.18637/jss.v100.i05>
- 832 Eddelbuettel, D., & Balamuta, J. J. (2018). Extending R with C++: A Brief Introduction  
833 to Rcpp. *The American Statistician*, 72(1), 28–36.  
834 <https://doi.org/10.1080/00031305.2017.1375990>
- 835 Eddelbuettel, D., & François, R. (2011). Rcpp: Seamless R and C++ integration. *Journal*  
836 *of Statistical Software*, 40(8), 1–18. <https://doi.org/10.18637/jss.v040.i08>
- 837 Gabry, J., Češnovar, R., Johnson, A., & Broder, S. (2024). *Cmdstanr: R interface to*  
838 *'CmdStan'*. Retrieved from <https://github.com/stan-dev/cmdstanr>
- 839 Gabry, J., Simpson, D., Vehtari, A., Betancourt, M., & Gelman, A. (2019). Visualization  
840 in bayesian workflow. *J. R. Stat. Soc. A*, 182, 389–402.  
841 <https://doi.org/10.1111/rssa.12378>
- 842 Gelman, A., Hill, J., & Vehtari, A. (2020). Regression and Other Stories.  
843 <https://www.cambridge.org/highereducation/books/regression-and-other-stories/DD20DD6C9057118581076E54E40C372C>; Cambridge University Press.  
844 <https://doi.org/10.1017/9781139161879>
- 845 Girard, J. (2024). *Standist: What the package does (one line, title case)*. Retrieved from  
846 <https://github.com/jmgirard/standist>

- 848 Grolemund, G., & Wickham, H. (2011). Dates and times made easy with lubridate.
- 849     *Journal of Statistical Software*, 40(3), 1–25. Retrieved from  
850     <https://www.jstatsoft.org/v40/i03/>
- 851 Halley, E. (1997). VI. An estimate of the degrees of the mortality of mankind; drawn from  
852     curious tables of the births and funerals at the city of Breslaw; with an attempt to  
853     ascertain the price of annuities upon lives. *Philosophical Transactions of the Royal*  
854     *Society of London*, 17(196), 596–610. <https://doi.org/10.1098/rstl.1693.0007>
- 855 Heiss, A. (2021, November 10). A Guide to Correctly Calculating Posterior Predictions  
856     and Average Marginal Effects with Multilevel Bayesian Models.  
857     <https://doi.org/10.59350/wbn93-edb02>
- 858 Holden, J. G., Van Orden, G. C., & Turvey, M. T. (2009). Dispersion of response times  
859     reveals cognitive dynamics. *Psychological Review*, 116(2), 318–342.  
860     <https://doi.org/10.1037/a0014849>
- 861 Hosmer, D. W., Lemeshow, S., & May, S. (2011). *Applied Survival Analysis: Regression*  
862     *Modeling of Time to Event Data* (2nd ed). Hoboken: John Wiley & Sons.
- 863 Ince, R. A., Paton, A. T., Kay, J. W., & Schyns, P. G. (2021). Bayesian inference of  
864     population prevalence. *eLife*, 10, e62461. <https://doi.org/10.7554/eLife.62461>
- 865 Kantowitz, B. H., & Pachella, R. G. (2021). The Interpretation of Reaction Time in  
866     Information-Processing Research 1. *Human Information Processing*, 41–82.  
867     <https://doi.org/10.4324/9781003176688-2>
- 868 Kay, M. (2023). *tidybayes: Tidy data and geoms for Bayesian models*.  
869     <https://doi.org/10.5281/zenodo.1308151>
- 870 Kelso, J. A. S., Dumas, G., & Tognoli, E. (2013). Outline of a general theory of behavior  
871     and brain coordination. *Neural Networks: The Official Journal of the International*  
872     *Neural Network Society*, 37, 120–131. <https://doi.org/10.1016/j.neunet.2012.09.003>
- 873 Kruschke, J. K., & Liddell, T. M. (2018). The Bayesian New Statistics: Hypothesis testing,  
874     estimation, meta-analysis, and power analysis from a Bayesian perspective.

- 875      *Psychonomic Bulletin & Review*, 25(1), 178–206.
- 876      <https://doi.org/10.3758/s13423-016-1221-4>
- 877      Kurz, A. S. (2023a). *Applied longitudinal data analysis in brms and the tidyverse* (version  
878      0.0.3). Retrieved from <https://bookdown.org/content/4253/>
- 879      Kurz, A. S. (2023b). *Statistical rethinking with brms, ggplot2, and the tidyverse: Second*  
880      *edition* (version 0.4.0). Retrieved from <https://bookdown.org/content/4857/>
- 881      Landes, J., Engelhardt, S. C., & Pelletier, F. (2020). An introduction to event history  
882      analyses for ecologists. *Ecosphere*, 11(10), e03238. <https://doi.org/10.1002/ecs2.3238>
- 883      Luce, R. D. (1991). *Response times: Their role in inferring elementary mental organization*  
884      (1. issued as paperback). Oxford: Univ. Press.
- 885      Makeham. (1860). *On the Law of Mortality and the Construction of Annuity Tables*. The  
886      Assurance Magazine, and Journal of the Institute of Actuaries.
- 887      McElreath, R. (2018). *Statistical Rethinking: A Bayesian Course with Examples in R and*  
888      *Stan* (1st ed.). Chapman and Hall/CRC. <https://doi.org/10.1201/9781315372495>
- 889      Meyer, D. E., Osman, A. M., Irwin, D. E., & Yantis, S. (1988). Modern mental  
890      chronometry. *Biological Psychology*, 26(1-3), 3–67.  
891      [https://doi.org/10.1016/0301-0511\(88\)90013-0](https://doi.org/10.1016/0301-0511(88)90013-0)
- 892      Müller, K., & Wickham, H. (2023). *Tibble: Simple data frames*. Retrieved from  
893      <https://CRAN.R-project.org/package=tibble>
- 894      Neuwirth, E. (2022). *RColorBrewer: ColorBrewer palettes*. Retrieved from  
895      <https://CRAN.R-project.org/package=RColorBrewer>
- 896      Panis, S. (2020). How can we learn what attention is? Response gating via multiple direct  
897      routes kept in check by inhibitory control processes. *Open Psychology*, 2(1), 238–279.  
898      <https://doi.org/10.1515/psych-2020-0107>
- 899      Panis, S., Moran, R., Wolkersdorfer, M. P., & Schmidt, T. (2020). Studying the dynamics  
900      of visual search behavior using RT hazard and micro-level speed–accuracy tradeoff  
901      functions: A role for recurrent object recognition and cognitive control processes.

- 902        *Attention, Perception, & Psychophysics*, 82(2), 689–714.
- 903        <https://doi.org/10.3758/s13414-019-01897-z>
- 904        Panis, S., Schmidt, F., Wolkersdorfer, M. P., & Schmidt, T. (2020). Analyzing Response  
905        Times and Other Types of Time-to-Event Data Using Event History Analysis: A Tool  
906        for Mental Chronometry and Cognitive Psychophysiology. *I-Perception*, 11(6),  
907        2041669520978673. <https://doi.org/10.1177/2041669520978673>
- 908        Panis, S., & Schmidt, T. (2016). What Is Shaping RT and Accuracy Distributions? Active  
909        and Selective Response Inhibition Causes the Negative Compatibility Effect. *Journal of*  
910        *Cognitive Neuroscience*, 28(11), 1651–1671. [https://doi.org/10.1162/jocn\\_a\\_00998](https://doi.org/10.1162/jocn_a_00998)
- 911        Panis, S., & Schmidt, T. (2022). When does “inhibition of return” occur in spatial cueing  
912        tasks? Temporally disentangling multiple cue-triggered effects using response history  
913        and conditional accuracy analyses. *Open Psychology*, 4(1), 84–114.  
914        <https://doi.org/10.1515/psych-2022-0005>
- 915        Panis, S., Torfs, K., Gillebert, C. R., Wagemans, J., & Humphreys, G. W. (2017).  
916        Neuropsychological evidence for the temporal dynamics of category-specific naming.  
917        *Visual Cognition*, 25(1-3), 79–99. <https://doi.org/10.1080/13506285.2017.1330790>
- 918        Panis, S., & Wagemans, J. (2009). Time-course contingencies in perceptual organization  
919        and identification of fragmented object outlines. *Journal of Experimental Psychology:  
920        Human Perception and Performance*, 35(3), 661–687.  
921        <https://doi.org/10.1037/a0013547>
- 922        Pedersen, T. L. (2024). *Patchwork: The composer of plots*. Retrieved from  
923        <https://CRAN.R-project.org/package=patchwork>
- 924        Pinheiro, J. C., & Bates, D. M. (2000). *Mixed-effects models in s and s-PLUS*. New York:  
925        Springer. <https://doi.org/10.1007/b98882>
- 926        R Core Team. (2024). *R: A language and environment for statistical computing*. Vienna,  
927        Austria: R Foundation for Statistical Computing. Retrieved from  
928        <https://www.R-project.org/>

- 929 Ripley, B., Venables, B., Bates, D. M., ca 1998), K. H. (partial. port, ca 1998), A. G.  
930 (partial. port, & polr), D. F. (support. functions for. (2024). *MASS: Support Functions*  
931 and *Datasets for Venables and Ripley's MASS*.
- 932 Singer, J. D., & Willett, J. B. (2003). *Applied Longitudinal Data Analysis: Modeling*  
933 *Change and Event Occurrence*. Oxford, New York: Oxford University Press.
- 934 Smith, P. L., & Little, D. R. (2018). Small is beautiful: In defense of the small-N design.  
935 *Psychonomic Bulletin & Review*, 25(6), 2083–2101.  
936 <https://doi.org/10.3758/s13423-018-1451-8>
- 937 Steele, F., Goldstein, H., & Browne, W. (2004). A general multilevel multistate competing  
938 risks model for event history data, with an application to a study of contraceptive use  
939 dynamics. *Statistical Modelling*, 4(2), 145–159.  
940 <https://doi.org/10.1191/1471082X04st069oa>
- 941 Teachman, J. D. (1983). Analyzing social processes: Life tables and proportional hazards  
942 models. *Social Science Research*, 12(3), 263–301.  
943 [https://doi.org/10.1016/0049-089X\(83\)90015-7](https://doi.org/10.1016/0049-089X(83)90015-7)
- 944 Townsend, J. T. (1990). Truth and consequences of ordinal differences in statistical  
945 distributions: Toward a theory of hierarchical inference. *Psychological Bulletin*, 108(3),  
946 551–567. <https://doi.org/10.1037/0033-2909.108.3.551>
- 947 Wickelgren, W. A. (1977). Speed-accuracy tradeoff and information processing dynamics.  
948 *Acta Psychologica*, 41(1), 67–85. [https://doi.org/10.1016/0001-6918\(77\)90012-9](https://doi.org/10.1016/0001-6918(77)90012-9)
- 949 Wickham, H. (2016). *ggplot2: Elegant graphics for data analysis*. Springer-Verlag New  
950 York. Retrieved from <https://ggplot2.tidyverse.org>
- 951 Wickham, H. (2023a). *Forcats: Tools for working with categorical variables (factors)*.  
952 Retrieved from <https://forcats.tidyverse.org/>
- 953 Wickham, H. (2023b). *Stringr: Simple, consistent wrappers for common string operations*.  
954 Retrieved from <https://stringr.tidyverse.org>
- 955 Wickham, H., Averick, M., Bryan, J., Chang, W., McGowan, L. D., François, R., ...

- 956 Yutani, H. (2019). Welcome to the tidyverse. *Journal of Open Source Software*, 4(43),  
957 1686. <https://doi.org/10.21105/joss.01686>
- 958 Wickham, H., Çetinkaya-Rundel, M., & Grolemund, G. (2023). *R for data science: Import,*  
959 *tidy, transform, visualize, and model data* (2nd edition). Beijing Boston Farnham  
960 Sebastopol Tokyo: O'Reilly.
- 961 Wickham, H., François, R., Henry, L., Müller, K., & Vaughan, D. (2023). *Dplyr: A*  
962 *grammar of data manipulation*. Retrieved from <https://dplyr.tidyverse.org>
- 963 Wickham, H., & Henry, L. (2023). *Purrr: Functional programming tools*. Retrieved from  
964 <https://purrr.tidyverse.org/>
- 965 Wickham, H., Hester, J., & Bryan, J. (2024). *Readr: Read rectangular text data*. Retrieved  
966 from <https://readr.tidyverse.org>
- 967 Wickham, H., Vaughan, D., & Girlich, M. (2024). *Tidyr: Tidy messy data*. Retrieved from  
968 <https://tidyr.tidyverse.org>
- 969 Winter, B. (2019). *Statistics for Linguists: An Introduction Using R*. New York:  
970 Routledge. <https://doi.org/10.4324/9781315165547>
- 971 Wolkersdorfer, M. P., Panis, S., & Schmidt, T. (2020). Temporal dynamics of sequential  
972 motor activation in a dual-prime paradigm: Insights from conditional accuracy and  
973 hazard functions. *Attention, Perception, & Psychophysics*, 82(5), 2581–2602.  
974 <https://doi.org/10.3758/s13414-020-02010-5>

975 **Supplementary material**976 **A. Definitions of discrete-time hazard, survivor, probability mass, and  
977 conditional accuracy functions**

978 The shape of a distribution of waiting times can be described in multiple ways (Luce,  
 979 1991). After dividing time in discrete, contiguous time bins indexed by  $t$ , let  $RT$  be a  
 980 discrete random variable denoting the rank of the time bin in which a particular person's  
 981 response occurs in a particular experimental condition. Because waiting times can only  
 982 increase, discrete-time EHA focuses on the discrete-time hazard function

$$983 \quad h(t) = P(RT = t | RT \geq t) \quad (1)$$

984 and the discrete-time survivor function

$$985 \quad S(t) = P(RT > t) = [1-h(t)].[1-h(t-1)].[1-h(t-2)] \dots [1-h(1)] \quad (2)$$

986 and not on the probability mass function

$$987 \quad P(t) = P(RT = t) = h(t).S(t-1) \quad (3)$$

988 nor the cumulative distribution function

$$989 \quad F(t) = P(RT \leq t) = 1-S(t) \quad (4)$$

990 The discrete-time hazard function of event occurrence gives you for each bin the  
 991 probability that the event occurs (sometime) in that bin, given that the event has not  
 992 occurred yet in previous bins. This conditionality in the definition of hazard is what makes  
 993 the hazard function so diagnostic for studying event occurrence, as an event can physically  
 994 not occur when it has already occurred before. While the discrete-time hazard function  
 995 assesses the unique risk of event occurrence associated with each time bin, the  
 996 discrete-time survivor function cumulates the bin-by-bin risks of event *nonoccurrence* to  
 997 obtain the probability that the event occurs after bin  $t$ . The probability mass function  
 998 cumulates the risk of event occurrence in bin  $t$  with the risks of event nonoccurrence in

999 bins 1 to  $t-1$ . From equation 3 we find that hazard in bin  $t$  is equal to  $P(t)/S(t-1)$ .

1000 For two-choice RT data, the discrete-time hazard function can be extended with the  
 1001 discrete-time conditional accuracy function

$$1002 \quad ca(t) = P(\text{correct} \mid RT = t) \quad (5)$$

1003 which gives you for each bin the probability that a response is correct given that it is  
 1004 emitted in time bin  $t$  (Allison, 2010; Kantowitz & Pachella, 2021; Wickelgren, 1977). This  
 1005 latter function is also known as the micro-level speed-accuracy tradeoff (SAT) function.

1006 The survivor function provides a context for the hazard function, as  $S(t-1) = P(RT >$   
 1007  $t-1) = P(RT \geq t)$  tells you on how many percent of the trials the estimate  $h(t) = P(RT =$   
 1008  $t \mid RT \geq t)$  is based. The probability mass function provides a context for the conditional  
 1009 accuracy function, as  $P(t) = P(RT = t)$  tells you on how many percent of the trials the  
 1010 estimate  $ca(t) = P(\text{correct} \mid RT = t)$  is based.

1011 While psychological RT data is typically measured in small, continuous units (e.g.,  
 1012 milliseconds), discrete-time EHA treats the RT data as interval-censored data, because it  
 1013 only uses the information that the response occurred sometime in a particular bin of time  
 1014  $(x,y]: x < RT \leq y$ . If we want to use the exact event times, then we treat time as a  
 1015 continuous variable, and let  $RT$  be a continuous random variable denoting a particular  
 1016 person's response time in a particular experimental condition. Continuous-time EHA does  
 1017 not focus on the cumulative distribution function  $F(t) = P(RT \leq t)$  and its derivative, the  
 1018 probability density function  $f(t) = F(t)'$ , but on the survivor function  $S(t) = P(RT > t)$   
 1019 and the hazard rate function  $\lambda(t) = f(t)/S(t)$ . The hazard rate function gives you the  
 1020 instantaneous *rate* of event occurrence at time point  $t$ , given that the event has not  
 1021 occurred yet.

1022 **B. Custom functions for descriptive discrete-time hazard analysis**

1023 We defined 13 custom functions that we list here.

- 1024 • censor(df,timeout,bin\_width) : divide the time segment  $(0, \text{timeout}]$  in bins, identify  
any right-censored observations, and determine the discrete RT (time bin rank)
  - 1025
  - 1026 • ptb(df) : transform the person-trial data set to the person-trial-bin data set
  - 1027
  - 1028 • setup\_lt(ptb) : set up a life table for each level of 1 independent variable
  - 1029
  - 1030 • setup\_lt\_2IV(ptb) : set up a life table for each combination of levels of 2  
independent variables
  - 1031
  - 1032
  - 1033 • calc\_ca(df) : estimate the conditinal accuracies when there is 1 independent variable
  - 1034
  - 1035 • calc\_ca\_2IV(df) : estimate the conditional accuraiies when there are 2 independent  
variables
  - 1036
  - 1037 • join\_lt\_ca(df1,df2) : add the  $\text{ca}(t)$  estimates to the life tables (1 independent  
variable)
  - 1038
  - 1039 • join\_lt\_ca\_2IV(df1,df2) : add the  $\text{ca}(t)$  estimates to the life tables (2 independent  
variables)
  - 1040
  - 1041
  - 1042
  - 1043
  - 1044
  - 1045
  - 1046
  - 1047
  - 1048
  - 1049
  - 1050
- extract\_median(df) : estimate quantiles  $S(t)._{50}$  (1 independent variable)
- extract\_median\_2IV(df) : estimate quantiles  $S(t)._{50}$  (2 independent variables)
- plot\_eha(df,subj,haz\_yaxis=1,first\_bin\_shown=1,aggregated\_data=F,Nsubj=6) :  
create plots of the discrete-time functions (1 independent variable), and specify the  
upper limit of the y-axis in the hazard plot, with which bin to start plotting, whether  
the data is aggregated across participants, and across how many participants
- plot\_eha\_2IV(df,subj,haz\_yaxis=1,first\_bin\_shown=1,aggregated\_data=F,  
Nsubj=6) : create plots of the discrete-time functions (2 independent variables), and  
specify the upper limit of the y-axis in the hazard plot, with which bin to start  
plotting, whether the data is aggregated across participants, and across how many  
participants

When you want to analyse simple RT data from a detection experiment with one  
independent variable, the functions calc\_ca() and join\_lt\_ca() should not be used, and  
the code to plot the conditional accuracy functions should be removed from the function

1051 plot\_eha(). When you want to analyse simple RT data from a detection experiment with  
1052 two independent variables, the functions calc\_ca\_2IV() and join\_lt\_ca\_2IV() should not  
1053 be used, and the code to plot the conditional accuracy functions should be removed from  
1054 the function plot\_eha\_2IV().

1055 **C. Link functions**

1056 Popular link functions include the logit link and the complementary log-log link, as  
1057 shown in Figure 15.

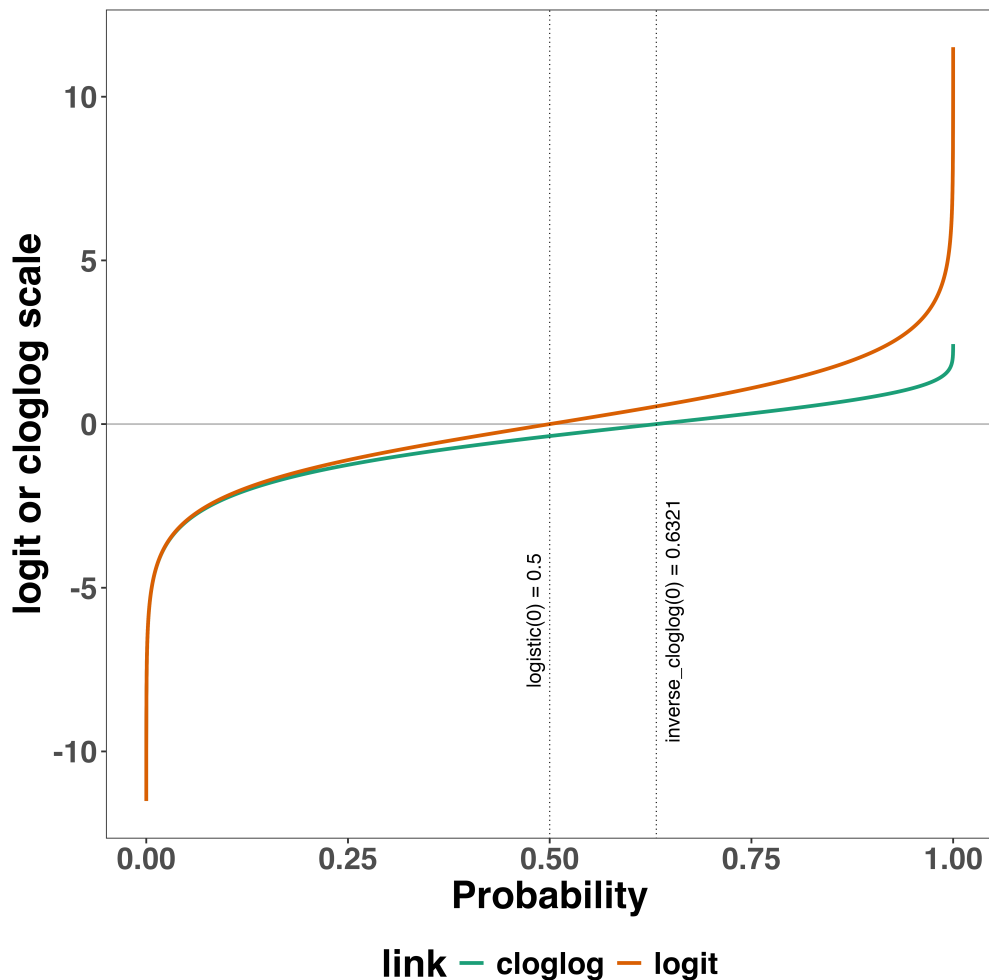


*Figure 15.* The logit and cloglog link functions.

1058 **D. Regression equations**

1059 An example (single-level) discrete-time hazard model with three predictors (TIME,  
 1060  $X_1$ ,  $X_2$ ), the cloglog link function, and a third-order polynomial specification for TIME can  
 1061 be written as follows:

$$\begin{aligned} 1062 \quad \text{cloglog}[h(t)] &= \ln(-\ln[1-h(t)]) = [\beta_0 \text{ONE} + \beta_1(\text{TIME}-9) + \beta_2(\text{TIME}-9)^2] + [\beta_3 X_1 + \beta_4 X_2 \\ 1063 &+ \beta_5 X_2(\text{TIME}-9)] \end{aligned} \quad (6)$$

1064 The main predictor variable TIME is the time bin index  $t$  that is centered on value 9  
 1065 in this example. The first set of terms within brackets, the parameters  $\beta_0$  to  $\beta_2$  multiplied  
 1066 by their polynomial specifications of (centered) time, represents the shape of the baseline  
 1067 cloglog-hazard function (i.e., when all predictors  $X_i$  take on a value of zero). The second  
 1068 set of terms (the beta parameters  $\beta_3$  to  $\beta_5$ ) represents the vertical shift in the baseline  
 1069 cloglog-hazard for a 1 unit increase in the respective predictor variable. Predictors can be  
 1070 discrete, continuous, and time-varying or time-invariant. For example, the effect of a 1 unit  
 1071 increase in  $X_1$  is to vertically shift the whole baseline cloglog-hazard function by  $\beta_1$   
 1072 cloglog-hazard units. However, if the predictor interacts linearly with TIME (see  $X_2$  in the  
 1073 example), then the effect of a 1 unit increase in  $X_2$  is to vertically shift the predicted  
 1074 cloglog-hazard in bin 9 by  $\beta_2$  cloglog-hazard units (when  $\text{TIME}-9 = 0$ ), in bin 10 by  $\beta_2 +$   
 1075  $\beta_3$  cloglog-hazard units (when  $\text{TIME}-9 = 1$ ), and so forth. To interpret the effects of a  
 1076 predictor, its  $\beta$  parameter is exponentiated, resulting in a hazard ratio (due to the use of  
 1077 the cloglog link). When using the logit link, exponentiating a  $\beta$  parameter results in an  
 1078 odds ratio.

1079 An example (single-level) discrete-time hazard model with a general specification for  
 1080 TIME (separate intercepts for each of six bins, where D1 to D6 are binary variables  
 1081 identifying each bin) and a single predictor ( $X_1$ ) can be written as follows:

$$1082 \quad \text{cloglog}[h(t)] = [\beta_0 D1 + \beta_1 D2 + \beta_2 D3 + \beta_3 D4 + \beta_4 D5 + \beta_5 D6] + [\beta_6 X_1] \quad (7)$$

**E. Prior distributions**

To gain a sense of what prior *logit* values would approximate a uniform distribution on the probability scale, Kurz (2023a) simulated a large number of draws from the Uniform(0,1) distribution, converted those draws to the log-odds metric, and fitted a Student's t distribution. Row C in Figure 12 shows that using a t-distribution with 7.61 degrees of freedom and a scale parameter of 1.57 as a prior on the logit scale, approximates a uniform distribution on the probability scale. According to Kurz (2023a), such a prior might be a good prior for the intercept(s) in a logit-hazard model, while the N(0,1) prior in row D might be a good prior for the non-intercept parameters in a logit-hazard model, as it gently regularizes p towards .5 (i.e., a zero effect on the logit scale).

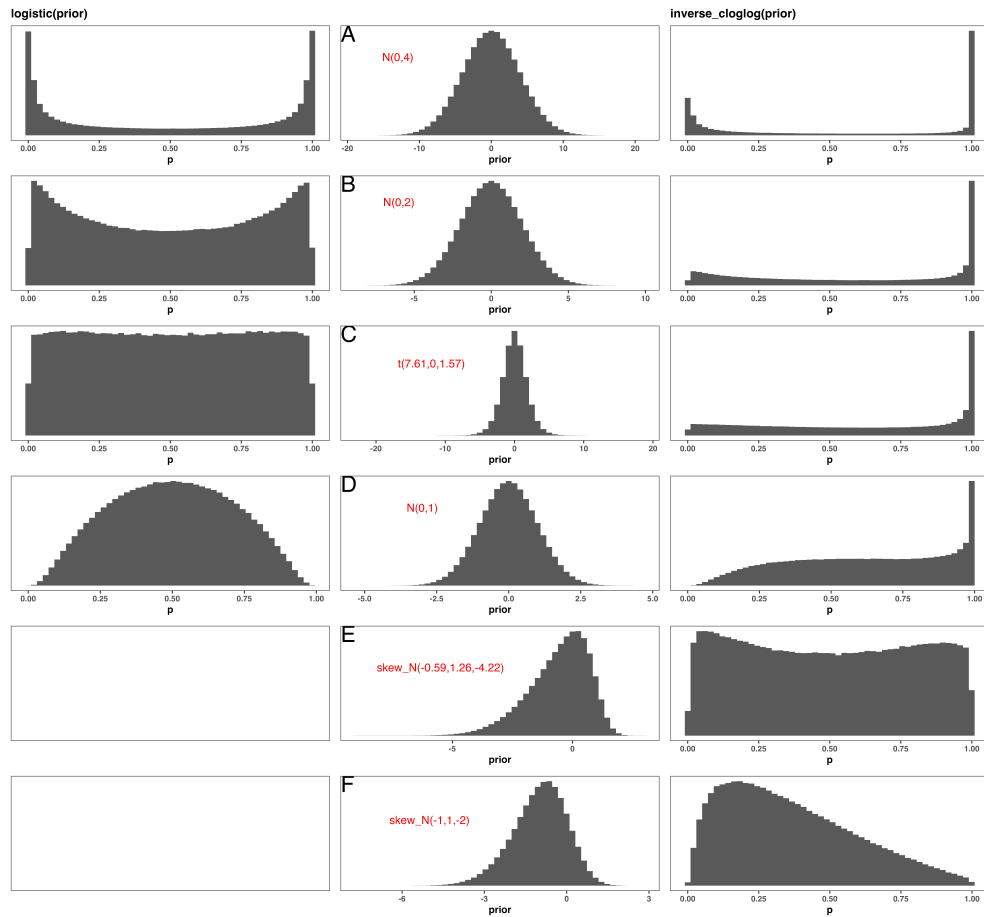


*Figure 16.* Prior distributions for the Intercept on the logit and/or cloglog scales (middle column), and their implications on the probability scale after applying the inverse-logit (or logistic) transformation (left column), and the inverse-cloglog transformation (right column).

1093 To gain a sense of what prior *cloglog* values would approximate a uniform distribution  
 1094 on the hazard probability scale, we followed Kurz's approach and simulated a large number  
 1095 of draws from the Uniform(0,1) distribution, converted them to the cloglog metric, and  
 1096 fitted a skew-normal model (due to the asymmetry of the cloglog link function). Row E  
 1097 shows that using a skew-normal distribution with a mean of -0.59, a standard deviation of  
 1098 1.26, and a skewness of -4.22 as a prior on the cloglog scale, approximates a uniform  
 1099 distribution on the probability scale. However, because hazard values below .5 are more  
 1100 likely in RT studies, using a skew-normal distribution with a mean of -1, a standard

1101 deviation of 1, and a skewness of -2 as a prior on the cloglog scale (row F), might be a good  
1102 weakly informative prior for the intercept(s) in a cloglog-hazard model. A skew-normal  
1103 distribution with a mean of -0.2, a standard deviation of 0.71, and a skewness of -2.2 might  
1104 be a good weakly informative prior for the non-intercept parameters in a cloglog-hazard  
1105 model as it gently regularizes p towards .6321 (i.e., a zero effect on the cloglog scale).

1106 **F. Advantages of hazard analysis**

1107 Statisticians and mathematical psychologists recommend focusing on the hazard  
1108 function when analyzing time-to-event data for various reasons. First, as discussed by  
1109 Holden, Van Orden, and Turvey (2009), “probability density [and mass] functions can  
1110 appear nearly identical, both statistically and to the naked eye, and yet are clearly different  
1111 on the basis of their hazard functions (but not vice versa). Hazard functions are thus more  
1112 diagnostic than density functions” (p. 331) when one is interested in studying the detailed  
1113 shape of a RT distribution (see also Figure 1 in Panis, Schmidt, et al., 2020). Therefore,  
1114 when the goal is to study how psychological effects change over time, hazard and  
1115 conditional accuracy functions are preferred.

1116 Second, because RT distributions may differ from one another in multiple ways,  
1117 Townsend (1990) developed a dominance hierarchy of statistical differences between two  
1118 arbitrary distributions A and B. For example, if  $h_A(t) > h_B(t)$  for all t, then both hazard  
1119 functions are said to show a complete ordering. Townsend (1990) concluded that stronger  
1120 conclusions can be drawn from data when comparing the hazard functions using EHA. For  
1121 example, when  $\text{mean } A < \text{mean } B$ , the hazard functions might show a complete ordering  
1122 (i.e., for all t), a partial ordering (e.g., only for  $t > 300$  ms, or only for  $t < 500$  ms), or they  
1123 may cross each other one or more times.

1124 Third, EHA does not discard right-censored observations when estimating hazard  
1125 functions, that is, trials for which we do not observe a response during the data collection

period in a trial so that we only know that the RT must be larger than some value (e.g., the response deadline). This is important because although a few right-censored observations are inevitable in most RT tasks, a lot of right-censored observations are expected in experiments on masking, the attentional blink, and so forth. In other words, by using EHA you can analyze RT data from experiments that typically do not measure response times. As a result, EHA can also deal with long RTs in experiments without a response deadline, which are typically treated as outliers and are discarded before calculating a mean. This orthodox procedure leads to underestimation of the true mean. By introducing a fixed censoring time for all trials at the end of the analysis time window, trials with long RTs are not discarded but contribute to the risk set of each bin.

Fourth, hazard modeling allows incorporating time-varying explanatory covariates such as heart rate, electroencephalogram (EEG) signal amplitude, gaze location, etc. (Allison, 2010). This is useful for linking physiological effects to behavioral effects when performing cognitive psychophysiology (Meyer et al., 1988).

Finally, as explained by Kelso, Dumas, and Tognoli (2013), it is crucial to first have a precise description of the macroscopic behavior of a system (here:  $h(t)$  and possibly  $ca(t)$  functions) in order to know what to derive on the microscopic level. EHA can thus solve the problem of model mimicry, i.e., the fact that different computational models can often predict the same mean RTs as observed in the empirical data, but not necessarily the detailed shapes of the empirical RT hazard distributions. Also, fitting parametric functions or computational models to data without studying the shape of the empirical discrete-time  $h(t)$  and  $ca(t)$  functions can miss important features in the data (Panis, Moran, et al., 2020; Panis & Schmidt, 2016).